





# Braincase and neuroanatomy of the lagerpetid *Dromomeron gregorii* (Archosauria, Pterosauroomorpha) with comments on the early evolution of the braincase and associated soft tissues in Avemetatarsalia

Mario Bronzati<sup>1</sup>  | Max C. Langer<sup>2</sup> | Martín D. Ezcurra<sup>3,4</sup>  |  
Michelle R. Stocker<sup>5,6</sup>  | Sterling J. Nesbitt<sup>5,6</sup> 

<sup>1</sup>Fachbereich Geowissenschaften der Eberhard Karls University Tübingen, Tübingen, Germany

<sup>2</sup>Departamento de Biologia, Universidade de São Paulo, Ribeirão Preto, SP, Brazil

<sup>3</sup>Sección Paleontología de Vertebrados, CONICET–Museo Argentino de Ciencias Naturales “Bernardino Rivadavia”, Buenos Aires, Argentina

<sup>4</sup>School of Geography, Earth and Environmental Sciences, University of Birmingham, Birmingham, UK

<sup>5</sup>Department of Geosciences, Virginia Tech, Blacksburg, Virginia, USA

<sup>6</sup>Vertebrate Paleontology Collection, The University of Texas at Austin, Austin, Texas, USA

## Correspondence

Mario Bronzati, Fachbereich  
Geowissenschaften der Eberhard Karls  
University Tübingen, Sigwartstraße 10,  
D-72076 Tübingen, Germany.  
Email: [mariobronzati@gmail.com](mailto:mariobronzati@gmail.com)

Sterling J. Nesbitt, Department of  
Geosciences, Virginia Tech, 926 West  
Campus Drive, Blacksburg,  
VA 24061, USA.  
Email: [sjn2104@vt.edu](mailto:sjn2104@vt.edu)

## Funding information

Agencia Nacional de Promoción Científica  
y Técnica, Grant/Award Number: PICT  
2018-01186; Alexander von Humboldt  
Foundation; National Science Foundation,  
Grant/Award Number: EAR 1943286; São  
Paulo Research Foundation (FAPESP),  
Grant/Award Numbers: 2014/03825-3,  
2018/18145-9; The Conselho Nacional de  
Desenvolvimento Científico e Tecnológico  
(CNPq), Grant/Award Number:  
170867/2017-0; Jackson School of  
Geosciences, University of Texas at Austin

## Abstract

The anatomy of the braincase and associated soft tissues of the lagerpetid *Dromomeron gregorii* (Archosauria: Avemetatarsalia) from the Late Triassic of the United States is here described. This corresponds to the first detailed description of cranial materials of Lagerpetidae, an enigmatic group of Late Triassic (c. 236–200 Million years ago) animals that are the closest known relatives of pterosaurs, the flying reptiles. The braincase of *D. gregorii* is characterized by the presence of an anteriorly elongated laterosphenoid and a postparietal, features observed in stem-archosaurs but that were still unknown in early members of the avian lineage of archosaurs. Using micro-computed tomography (CT-scan data), we present digital reconstructions of the brain and endosseous labyrinth of *D. gregorii*. The brain of *D. gregorii* exhibits a floccular lobe of the cerebellum that projects within the space of the semicircular canals. The semicircular canals are relatively large when compared to other archosaur-omorphs, with the anterior canal exhibiting a circular shape. These features of the sensory structures of *D. gregorii* are more similar to those of pterosaurs than to those of other early avemetatarsalians. In sum, the braincase anatomy of *D. gregorii* shows a combination of plesiomorphic and apomorphic features in the phylogenetic context of Archosauria and suggests that the still poorly

This is an open access article under the terms of the [Creative Commons Attribution-NonCommercial-NoDerivs](https://creativecommons.org/licenses/by-nc-nd/4.0/) License, which permits use and distribution in any medium, provided the original work is properly cited, the use is non-commercial and no modifications or adaptations are made.

© 2023 The Authors. *The Anatomical Record* published by Wiley Periodicals LLC on behalf of American Association for Anatomy.

understood early evolution of the braincase in avemetatarsalians is complex, with a scenario of independent acquisitions and losses of character states.

#### KEYWORDS

braincase, Dromomeron, Lagerpetidae, Pterosauroomorpha, sensory systems

## 1 | INTRODUCTION

Lagerpetidae is a clade of small and enigmatic forms within Avemetatarsalia (=Pan-Aves sensu Ezcurra et al., 2020), the lineage of Archosauria including birds (Serenó, 1991). These animals were previously understood as non-dinosaurian dinosauromorphs (e.g., Cabreira et al., 2016; Ezcurra, 2016; Irmis et al., 2007; Nesbitt, 2011; Novas, 1996; Sereno & Arcucci, 1993), but recent phylogenetic hypotheses indicate that lagerpetids are the closest relatives of pterosaurs (Figure 1; Baron, 2021; Ezcurra et al., 2020; Foffa et al., 2022; Kellner et al., 2022; Müller et al., 2023). Lagerpetid fossils have been found in Upper Triassic (around 236–200 Ma) deposits of North- (e.g., Irmis et al., 2007; Nesbitt, Irmis, et al., 2009) and South America (e.g., Cabreira et al., 2016; Martínez et al., 2016; Romer, 1971; Arcucci, 1986), in Middle/Late Triassic beds of Madagascar (Kammerer et al., 2020), and perhaps in the Late Triassic of Scotland (Foffa et al., 2022). Their stratigraphic age and phylogenetic position as close relatives of either pterosaurs or dinosaurs are critical to understand the anatomy and early evolution of avemetatarsalians.

A series of studies conducted in the last 15 years have documented the anatomy of lagerpetids (Cabreira et al., 2016; Ezcurra et al., 2020; Irmis et al., 2007; Kammerer et al., 2020; Martínez et al., 2016; Nesbitt, Smith, et al., 2009), but their cranial anatomy is known in much less detail than their postcranial skeleton. The recovered lagerpetid remains are mostly represented by postcranial elements (vertebral series and limbs), with much scarcer cranial parts. Furthermore, the rare cranial materials of

lagerpetids have only been briefly described (see Cabreira et al., 2016; Ezcurra et al., 2020; Kammerer et al., 2020). To reduce this gap, we provide the first detailed osteological description of a lagerpetid skull part (see Figures 2–7), the braincase and partial skull table (frontals, parietals) of *Dromomeron gregorii* (TMM 31100-1334; see Institutional Abbreviations) from the Late Triassic of the USA (Nesbitt, Smith, et al. 2009). Based on data from micro-Computed Tomography (CT-scan data), we also describe soft-tissue reconstructions associated with it, including the brain, inner ear, cranial nerves, and blood vessels (see Figure 8).

## 2 | MATERIALS AND METHODS

### 2.1 | Institutional abbreviations

BPI, Evolutionary Studies Institute (formerly Bernard Price Institute for Palaeontological Research), University of the Witwatersrand, Johannesburg, South Africa; CAPPA/UFSM, Centro de Apoio à Pesquisa Paleontológica da Quarta Colônia, Universidade Federal de Santa Maria, São João do Polêsine, Brazil; GR, Ghost Ranch Ruth Hall Museum of Palaeontology, Abiquiu, USA; MB, Museum für Naturkunde, Berlin, Germany; MCP PV, Museu de Ciências e Tecnologia, Pontifícia Universidade Católica do Rio Grande do Sul, Porto Alegre, Brazil; IGO-V, Museo Mario Sánchez Roig, Instituto de Geología y Paleontología, La Habana, Cuba; MPEF, Museo Paleontológico Egidio Feruglio, Trelew, Argentina; MSM, Mesa Southwest Museum, Mesa, Arizona, USA; NHMUK, Natural History Museum, Palaeontology Vertebrates, London, United Kingdom; NMT,

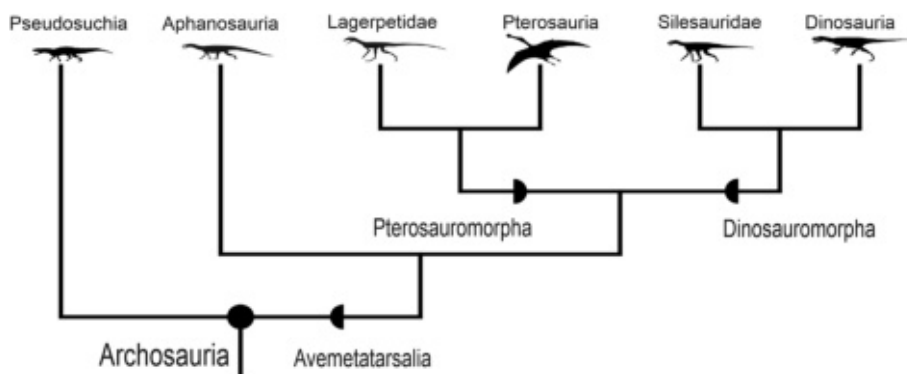
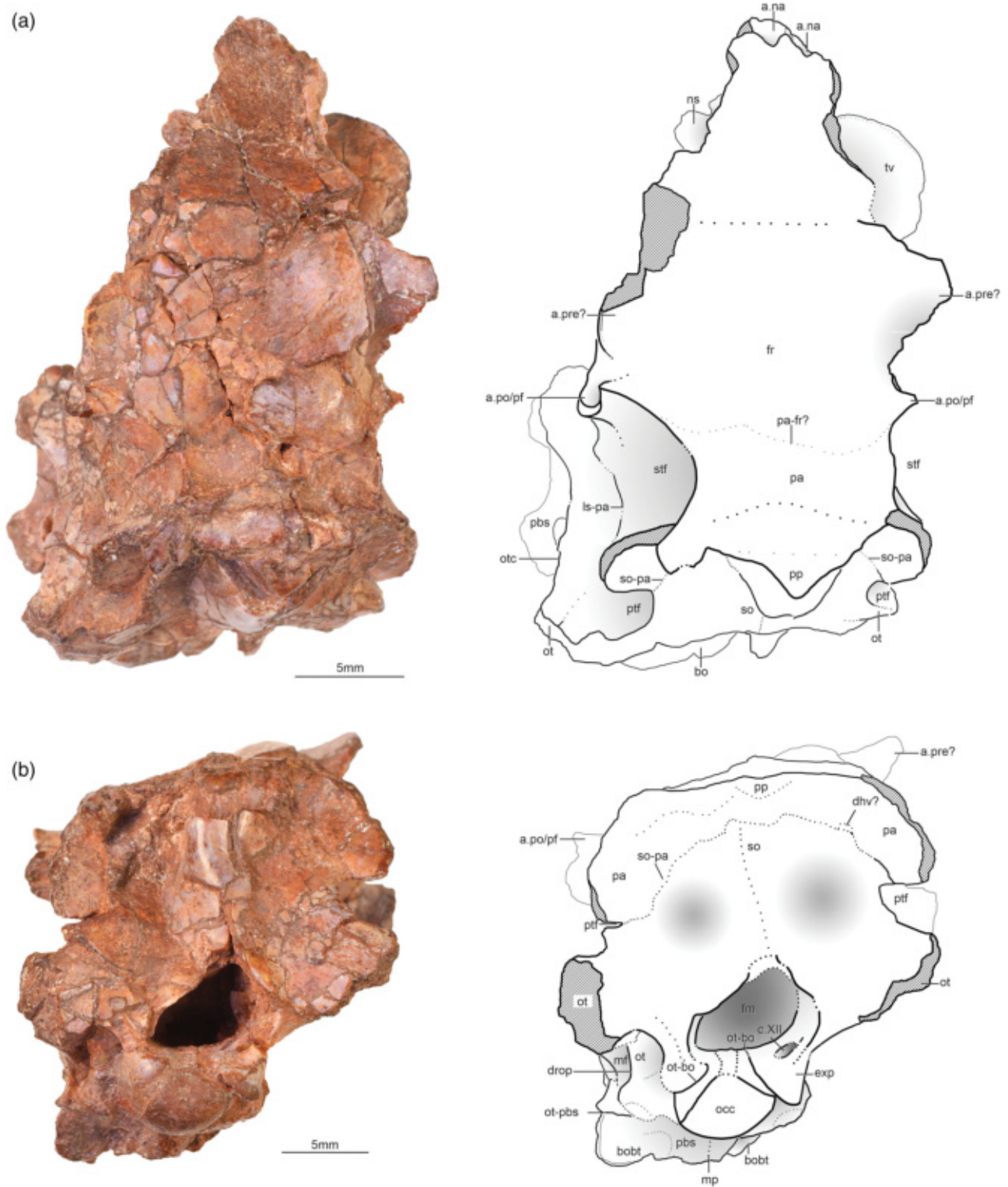


FIGURE 1 Simplified phylogeny of Archosauria and the position of Lagerpetidae within Avemetatarsalia.



**FIGURE 2** The braincase of specimen TMM 31100-1334 of *Dromomeron gregorii* in dorsal and posterior views. (a) Photograph of the braincase in dorsal view on the left and interpretative drawing on the right; (b) photograph of the braincase in posterior view on the left and interpretative drawing on the right. a., articulates with; bo, basioccipital; bobt, basioccipital basitubera; c.XII, foramina for cranial nerve XII (hypoglossal); dhv, dorsal head vein; drop, descending process of the opisthotic; exp, exoccipital pillar; fr, frontal; ls-pa, suture between the laterosphenoid and parietal; mf, metotic foramen; mp, medial protuberance; na, nasal; ns, neural spine; occ, occipital condyle; ot, otoccipital; otc, otosphenoidal crest; ot-bo, suture between the otoccipital and basioccipital; ot-pbs, suture between the otoccipital and parabasisphenoid; pa, parietal; pbs, parabasisphenoid; po/pf, postorbital or postfrontal; pp, postparietal; pre?, prefrontal?; ptf, post-temporal fenestra; so, supraoccipital; stf, supratemporal fenestra so-pa, suture between the supraoccipital and parietal; tv, trunk vertebra.

National Museum of Tanzania, Dar es Salaam, Tanzania; PVL, Paleontologia de Vertebrados, Instituto “Miguel Lillo,” San Miguel de Tucumán, Argentina; PVSJ, Instituto y Museo de Ciencias Naturales, San Juan, Argentina; PULR, Universidad Nacional de La Rioja, La Rioja, Argentina; QG, Natural History Museum of Zimbabwe, Bulawayo, Zimbabwe; SAM, Iziko South African Museum, Capetown, South Africa; SMNS, Staatliches Museum für Naturkunde, Stuttgart, Germany; TMM, Collections at the Vertebrate Paleontology Laboratory (former Texas Memorial Museum), Austin, Texas, USA; ULBRA-PV, Centro de Apoio à Pesquisa Paleontológica da Quarta Colônia/Universidade Federal de Santa Maria, São João do Polêsine, Rio Grande do Sul, Brazil (previously Museu de Ciências Naturais, Universidade Luterana do Brasil, Canoas, Brazil); ZPAL, Institute of Paleobiology of the Polish Academy of Sciences, Warsaw, Poland.

## 2.2 | The partial skull of *Dromomeron gregorii*—TMM 31100-1334

Here, we follow the rationale detailed by Ezcurra et al. (2020) to assign TMM 31100-1334 to *D. gregorii*. The specimen was collected from Otis Chalk Quarry 3 (TMM 31100) between the years 1939 and 1941 (Stocker, 2013), but remained unprepared for more than 70 years. A small unprepared block of bone and rock containing the partial skull and 12 loose and unprepared vertebrae were found in a box among other unprepared fossils from TMM 31100. After full preparation of the vertebrae and skull, we discovered that a small piece of the frontal was still attached to one of the trunk vertebrae, confirming that the vertebrae, together with the skull in the box, were directly associated with the skull in the field. Furthermore, other specimens found by the same field crew at the same time were carefully collected, and associated material was kept together by wrapping them all together. This wrapped material was placed into individual boxes in the early 2000s, where it was discovered by our team in 2009.

The skull and vertebrae (TMM 31100-1334) were also discovered in the same drawer containing the holotype of *D. gregorii* (Nesbitt, Irmis, et al., 2009), a complete right femur (TMM 31100-1306). It is uncertain if the femur was found directly associated with the skull because this information from the original reports of the Work Progress Administration (USA) for this particular material was never recorded. However, the proximity of the femur to the skull and vertebrae in the drawer, which was organized by field number, may indicate that the specimens were found within a few days of each other at a minimum. The preservation of the femur and skull and vertebrae are similar in that they have well preserved surfaces with little calcium carbonate coating and the red mudstone matrix was the

same (SJN, personal observation based on preparation of the specimens). Beyond the collection of the specimens, the femur to skull size is consistent when comparing to other lagerpetids [e.g., *Ixalerpeton polesinensis* (ULBRA-PVT059) and *Ventoraptor gassenae* (Müller et al., 2023)]. Additionally, the similarity of the braincase described here with that found in association with a closely related lagerpetid, *I. polesinensis*, indicates that the braincase indeed belongs to a lagerpetid. Shared traits include: foramen for the trigeminal nerve formed solely by the prootic, without contribution of the laterosphenoid; frontal tapping anteriorly; similar general architecture of the endosseous labyrinth of the inner ear as demonstrated by geometric morphometrics analyses of the semicircular canals (see Bronzati et al., 2021).

The skull of *D. gregorii* now consists of two pieces, one piece with nearly all of the braincase and skull components and one piece that includes the anterior portion of the right frontal and an adhered trunk vertebra. During initial preparation and description of the skull, the anterior portion of the frontal and the adhered vertebra had not been identified, so during the CT-scanning of specimen, the anterior portion and the vertebra are not included. The anterior portion of the frontal and vertebra were adhered to the rest of the skull with B-72 (i.e., reversible) so that this portion can be removed in the future to observe the front of the laterosphenoids; we have provided figures both with (Figures 2, 3, and 5) and without (Figures 4 and 7) the anterior portion of the frontal and vertebra in place.

## 2.3 | CT-scan procedure

TMM 31100-1334 was scanned at the University of Texas High-Resolution X-ray CT Facility (voltage: 210 kV; current: 0.12 mA; voxel size 0.02832 mm X, 0.02832 mm Y, 0.06136 mm Z). From this scan, a total of 581 slices were generated. The three models presented here were generated by manual segmentation in the software Amira (version 5.3.3, Visage Imaging, Berlin, Germany). CT data are available through MorphoSource (<https://www.morphosource.org/projects/000535758>).

## 3 | RESULTS

We primarily compared the braincase anatomy of TMM 31100-1334 with that of the Brazilian lagerpetid *I. polesinensis* (ULBRA-PVT059) because it is the only other lagerpetid with comparable skull material (*V. gassenae* was published after this paper went to review). Yet, in order to provide a clearer scenario of braincase evolutionary patterns along the rise of



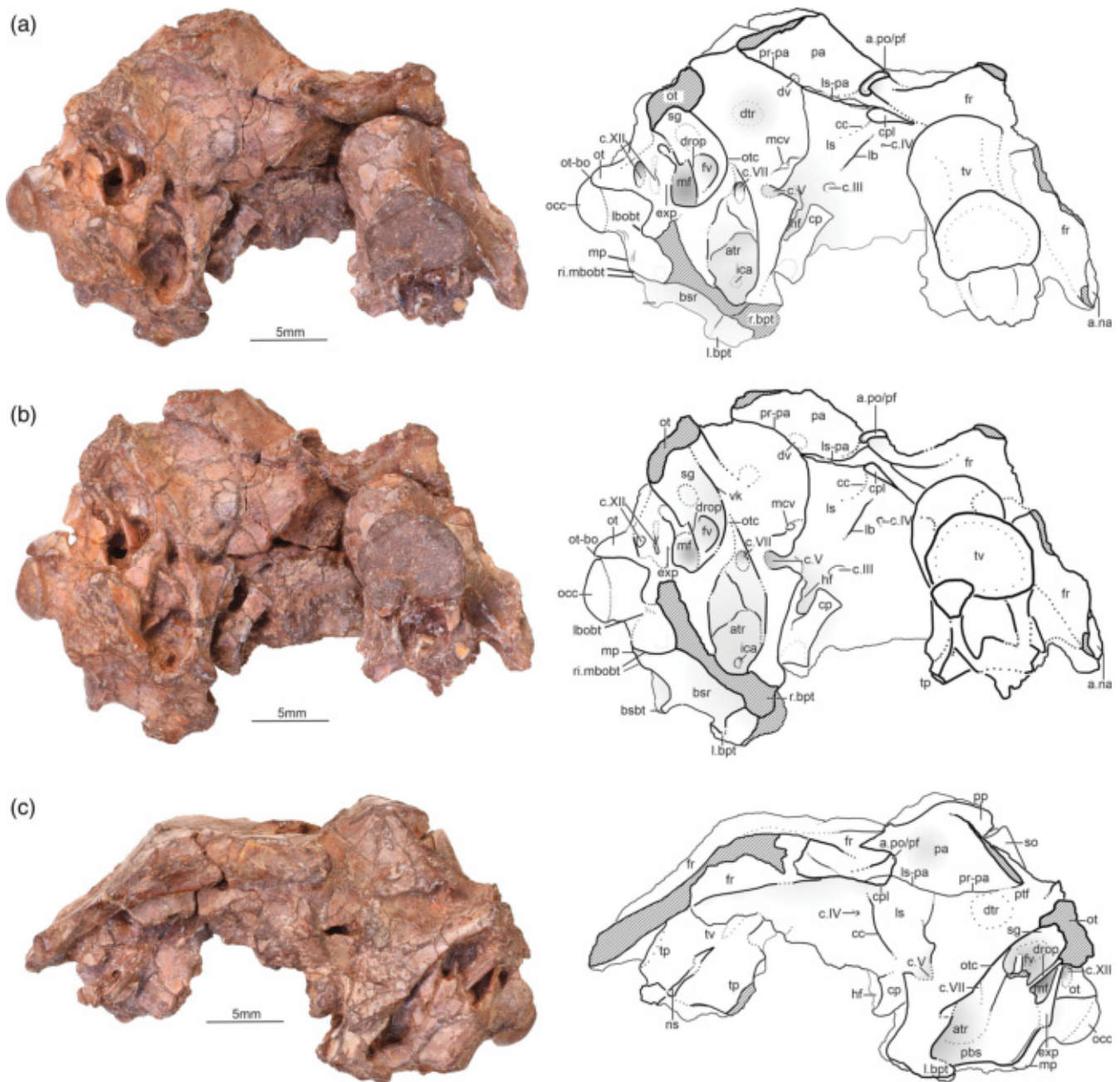


**FIGURE 3** The brainscase of specimen TMM 31100-1334 of *Dromomeron gregorii* in left and right lateral views. (a) Photograph of the brainscase in right lateral view on the left and interpretative drawing on the right; (b) photograph of the brainscase in right lateroventral view on the left and interpretative drawing on the right; (c) photograph of the brainscase in left lateral view on the left and interpretative drawing on the right. a., articulates with; atr, anterior tympanic recess; bpt, basiptyergoid process; bsr basisphenoid recess; c.III, foramen for cranial nerve III (oculomotor); c.IV, foramen for cranial nerve IV (trochlear); c.V, foramen for cranial nerve V (trigeminal); c.VII, foramen for cranial nerve VII (facial); c.XII, foramina for cranial nerve XII (hypoglossal); cc, cotylar crest; cp, cultriform process of the parabasisphenoid; cpl, capitata process of the laterosphenoid; drop, descending process of the opisthotic/crista infenestralis; dtr, dorsal tympanic recess; dv, dorsal head vein; exp, exoccipital pillar; fr, frontal; fv, fenestra vestibuli; hf, hypophyseal (pituitary) fossa; ica, entry for the internal carotid artery; l., left; lb, laterosphenoid buttress; lbobt, lateral component of the basioccipital basitubera; bsbt, basisphenoid basitubera; ls, laterosphenoid; ls-pa, suture between the laterosphenoid and parietal; mcv, mid-cerebral vein; mbobt, medial component of the basioccipital basitubera; mf, metotic foramen; mp, medial protuberance; na, nasal; ns, neural spine; occ, occipital condyle; ot, otoccipital; ot-bo, suture between the otoccipital and basioccipital; otc, otosphenoidal crest; pa, parietal; pbs, parabasisphenoid; po/pf, postorbital or postfrontal; pp, postparietal?; pr-pa, suture between the prootic and parietal; ptf, post-temporal fenestra; r., right; ri., ridge; sg, stapedia groove; tp, transverse process; tv, trunk vertebra; vk, ventral keel.

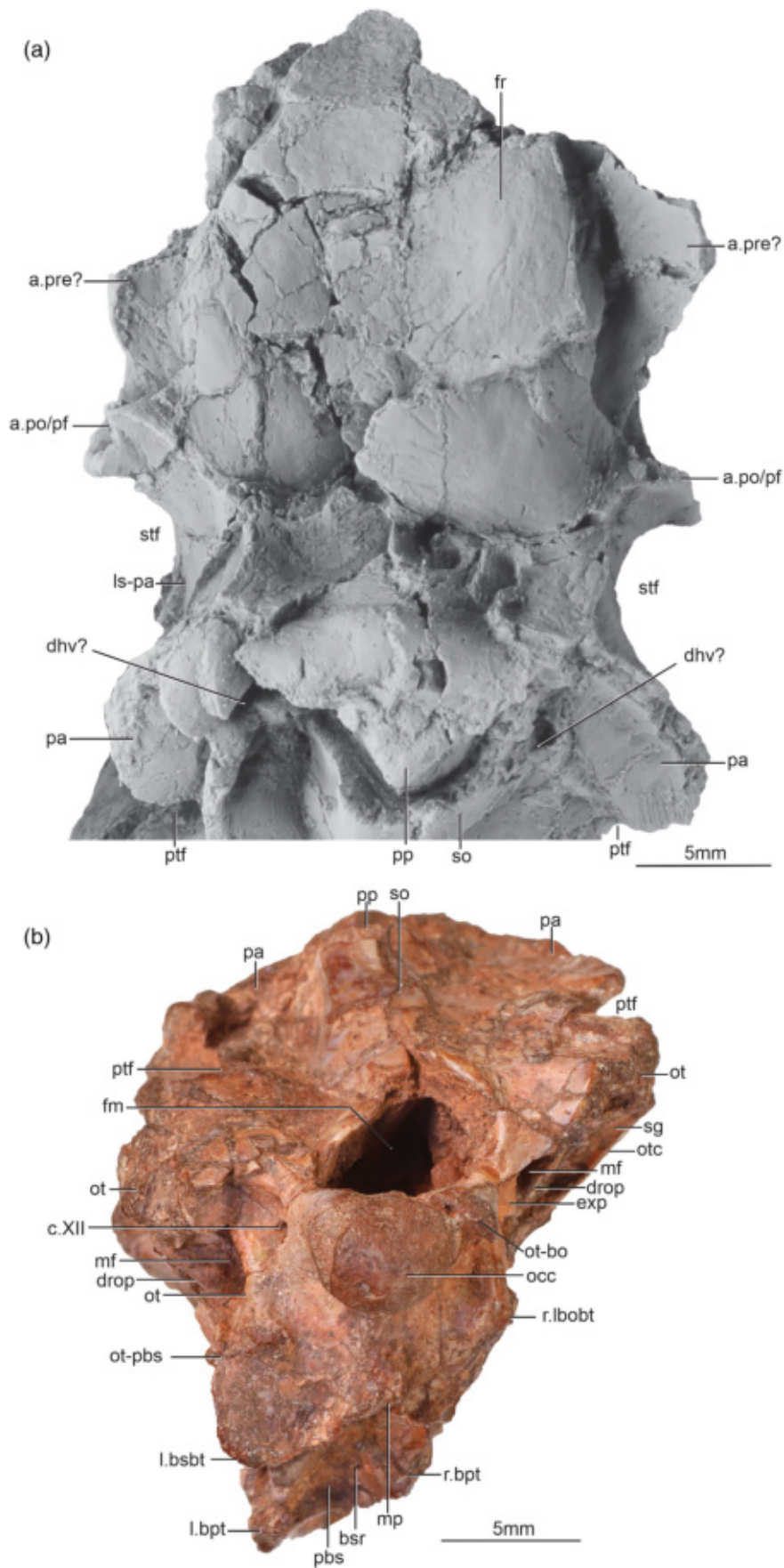
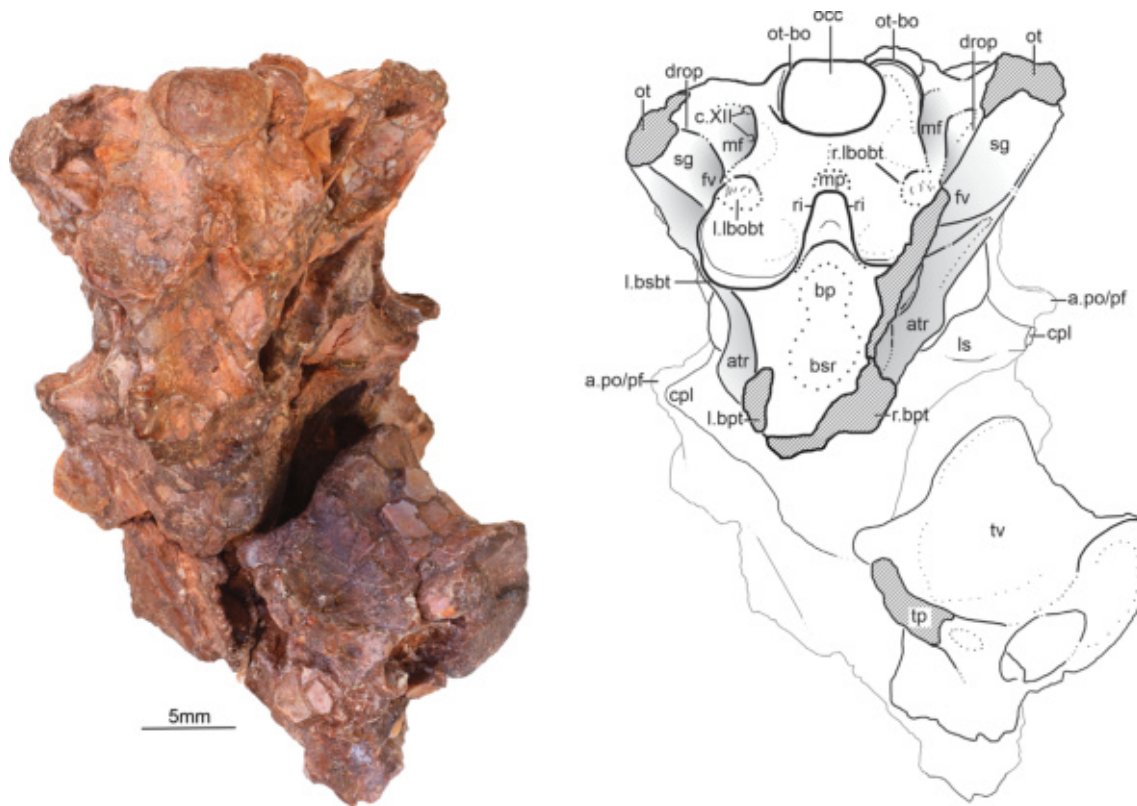


FIGURE 4 Legend on next page.



**FIGURE 5** The braincase of specimen TMM 31100-1334 of *Dromomeron gregorii* in ventral view. Photograph of the braincase in ventral view on the left, and interpretative drawing of the braincase in ventral view on the right. a, articulation; atr, anterior tympanic recess; bp, blind pit; bpt, basiptyergoid process; bsbt, basisphenoid basitubera; bsr, basisphenoid recess; cpl, capitate process of the laterosphenoid; c.XII, foramina for cranial nerve XII (hypoglossal); drop, descending ramus of the opisthotic; fv, fenestra vestibuli; l, left; lbobt, lateral component of the basioccipital basitubera; ls, laterosphenoid; mf, metotic foramen; mp, medial protuberance; occ, occipital condyle; ot, otoccipital; pf, postfrontal; po, postorbital; r, right; ri, ridge; sg, stapedial groove; tp, transverse process; tv, trunk vertebra.

Avemetatarsalia, we also employed braincases of stem-archosaurs, early pseudosuchians (Pan Crocodylia), early dinosauromorphs, and pterosaurs in the comparisons (Table 1 for a detailed list of taxa).

### 3.1 | General aspects of the braincase and skull roof of TMM 31100-1334

The braincase of *D. gregorii* (TMM 31100-1334) has all its elements preserved, including basioccipital, parabasi-sphenoid (parasphenoid + basisphenoid), supraoccipital,

otoccipitals (exoccipital + opisthotic), prootics, and laterosphenoids (Figures 2 and 3). Skull roof bones including the frontals, parietals, and a postparietal remain articulated to the braincase. All these elements are preserved in near natural articulation with one another, but some distortion is obvious (e.g., the anterior portion of the braincase elements is collapsed, Figure 2). If the basioccipital is horizontally aligned, the dorsal portion of the braincase and the skull roof are laterally twisted, in a way that the lateral margin of the left orbital rim is ventrally located in relation to the right (Figure 3). Indeed, the mid-sagittal plane of the dorsal portion of the braincase and skull roof

**FIGURE 4** The braincase of specimen TMM 31100-1334 of *Dromomeron gregorii* in dorsal and occipital views. (a) Photograph of the braincase in dorsal view; (b) photograph of the braincase in occipital view. a., articulation; bpt, basiptyergoid process; bsr, basisphenoid recess; bsbt, basisphenoid basitubera; c.XII, foramina for cranial nerve XII (hypoglossal); dhv, dorsal head vein; drop, descending process of the opisthotic/crista infenestralis; exp, exoccipital pillar; fm, foramen magnum; fr, frontal; l, left; lbobt, lateral component of the basioccipital basitubera; ls, laterosphenoid; mf, metotic foramen; mp, medial protuberance; occ, occipital condyle; ot, otoccipital; otc, otosphenoidal crest; ot-bo, suture between otoccipital and basioccipital; pa, parietal; pbs, parabasisphenoid; po/pf, postorbital/postfrontal; pp, postparietal; pre?, prefrontal?; ptf, post-temporal fenestra; r., right; sg, stapedial groove; so, supraoccipital; stf, supratemporal fenestra.



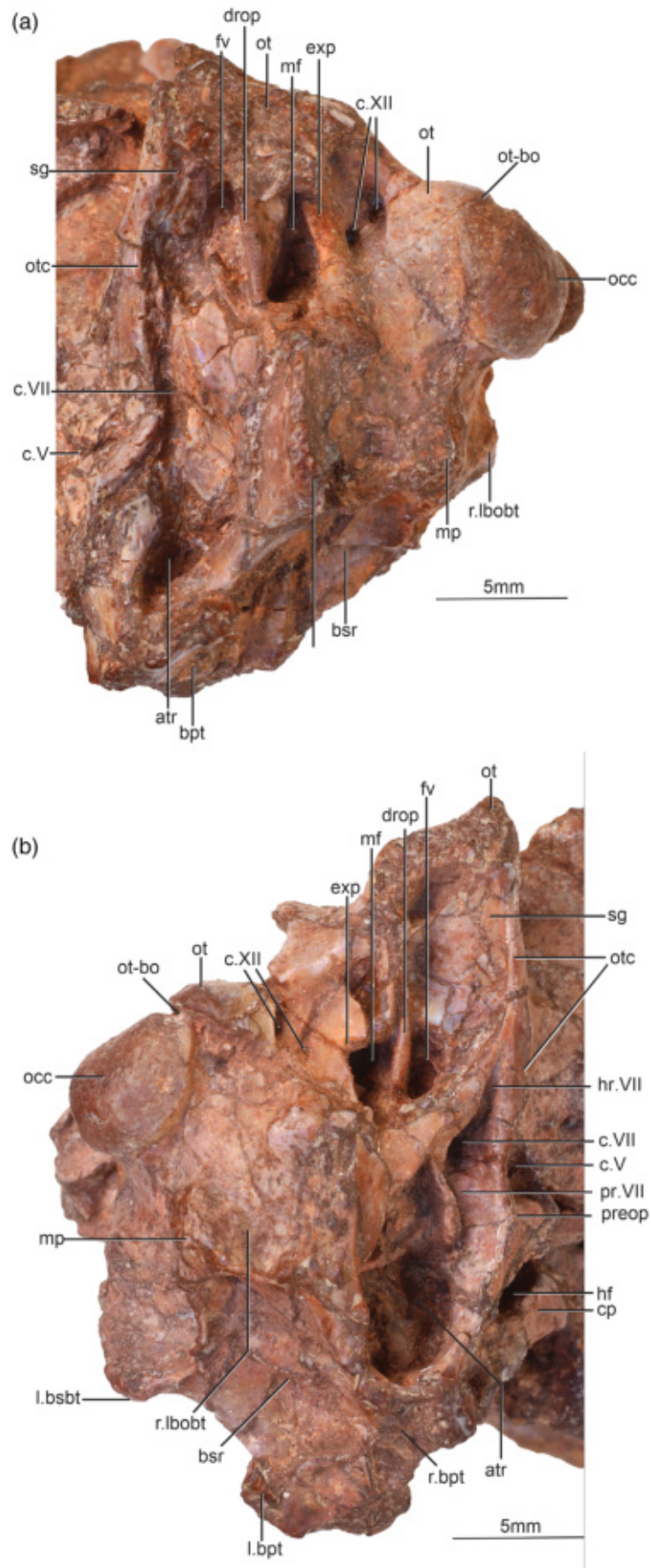
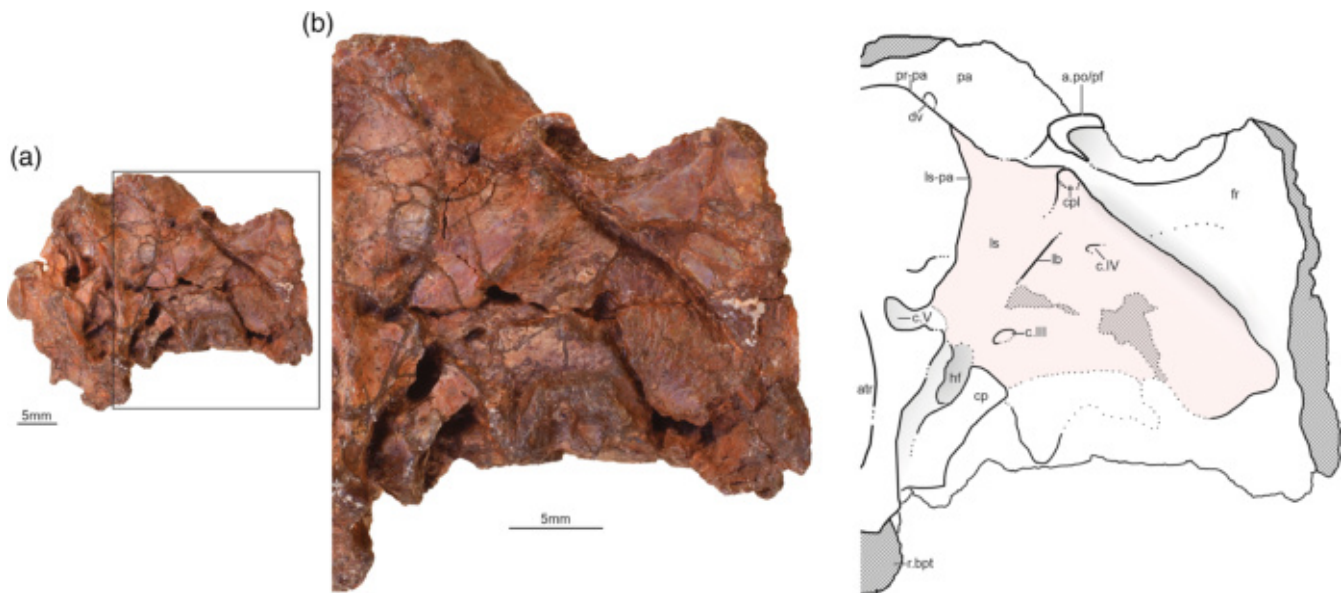


FIGURE 6 Legend on next page.





**FIGURE 7** The braincase of specimen TMM 31100-1334 of *Dromomeron gregorii* in right lateral view with trunk vertebra removed to expose the lateral surface of the laterosphenoid. (a) Photograph of the braincase in right lateral view. (b) Close-up of the lateral surface of the laterosphenoid on the left, and interpretative drawing of the laterosphenoid on the right. a.po/pf, articulation with postorbital or postfrontal; atr, anterior tympanic recess; bpt, basiptyergoid process; cp, cultriform process of the basisphenoid; cpl, capitate process of the laterosphenoid; c.III, foramen for cranial nerve III (oculomotor); c.IV, foramen for cranial nerve IV (trochlear); c.V, foramen for cranial nerve V (trigeminal); dv, dorsal head vein; hf, hypophyseal fossa; lb, laterosphenoid buttress; fr, frontal; ls, laterosphenoid; pa, parietal pr.pa, articulation between prootic and parietal; r, right.

is displaced to the right side in relation to the same plane in the ventral portion of the braincase. CT data helped trace nerve, inner ear, and vascular passages, and other external features of the bones, but the inner surfaces of elements (i.e., surfaces forming the endocranial cavity) were not easily discernible from the matrix. The CT data aided with the recognition of some suture lines between some of the bones (e.g., basioccipital-parabasisphenoid), but most of the sutures remained impossible to confidently identify. Therefore, we focused on the structures typically associated with individual braincase elements in archosauromorphs, rather than on attempting to describe the exact shape of each element.

The preserved braincase and skull roof of TMM 31100-1334 is 40.3 mm long from the posterior tip of the basioccipital to the anteriormost preserved part of the frontals (Figures 2 and 3). It is 22.7 mm tall, from the

ventral edge of the parabasisphenoid component of the basitubera to the dorsal extent of the parietals midline (Figure 3). The foramen magnum has a maximum width of 6 mm at its ventral portion. This seems less distorted than the dorsal portion, which is laterally displaced to the right. The foramen magnum height is approximately the same as its width.

### 3.2 | Skull roof

The preserved skull roof of TMM 31100-1334 is formed by the frontals, parietals, and by a postparietal. Sutures between the bones (including those between the left and right parietals and frontals) are not distinguishable on the outer surface of the skull roof, except for that between the postparietal and parietals (Figures 2 and 4).

**FIGURE 6** The braincase of specimen TMM 31100-1334 of *Dromomeron gregorii*—details of the otic and occipital region. (a) Photograph of the braincase in left lateral view; (b) photograph of the braincase in right lateral view. atr, anterior tympanic recess; bpt, basiptyergoid process; bsbt, basisphenoid basitubera; bsr, basisphenoid recess; c.V, foramen for cranial nerve V (trigeminal); c.VII, foramen for cranial nerve VII (facial); c.XII, foramina for cranial nerve XII (hypoglossal); cp, cultriform process; drop, descending process of the opisthotic/crista interfenestralis; exp, exoccipital pillar; fv, fenestra vestibuli; hf, hypophyseal (pituitary) fossa; hr.VII, groove associated with the hyomandibular ramus of the facial nerve; l., left; llobt, lateral component of the basioccipital basitubera; mf, metotic foramen; mp, medial protuberance; occ, occipital condyle; ot, otoccipital; otc, otosphenoidal crest; ot-bo, suture between otoccipital and basioccipital; preop, preotic pendant; pr.VII, groove associated with the palatine ramus of the facial nerve; r., right; sg, stapedial groove.

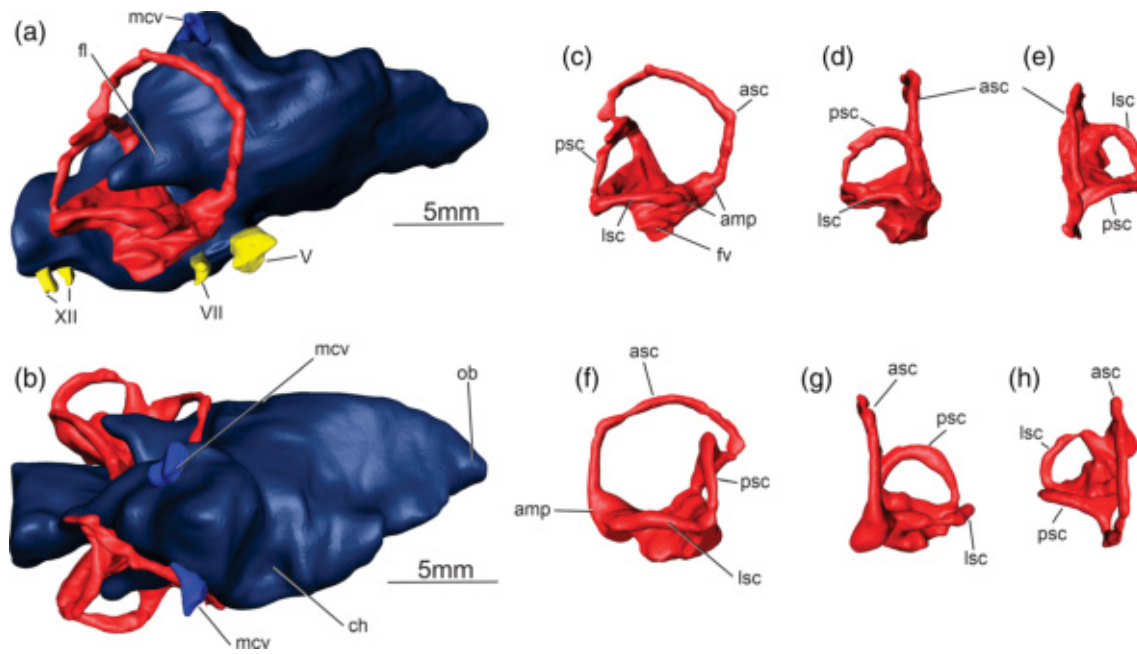


**FIGURE 8** Digital cranial endocast of specimen TMM 31100-1334 of *Dromomeron gregorii*. (a) endocast in right lateral view; (b) endocast in dorsal view; (c–e) right labyrinth in lateral, anterior and dorsal views, respectively; (f–h) left labyrinth in lateral, anterior and dorsal views, respectively. amp, ampulla; asc, anterior semicircular canal; ch, cerebral hemisphere; fl, floccular lobe of the cerebellum; fv, fenestra vestibuli; lsc, lateral semicircular canal; mcv, mid-cerebral vein; ob, olfactory bulb; psc, posterior semicircular canal; V, trigeminal nerve; VII, facial nerve; XII, hypoglossal nerve.

The maximum width of the skull roof of TMM 31100-1334 is nearly 19.8 mm, at the level of the anterior limit of the supratemporal fenestrae and the posterior limit of the orbit. At the dorsalmost portion of the orbit (anterior to its posterior limit), the skull roof is approximately half its maximum width, that is, approximately 9.7 mm (measured where the frontals are most complete). This narrowing is mostly related to a great anterior decrease in the width of the frontals, as seen in *I. polesinensis* (ULBRA-PVT059) and in the pterosaur *Allkaruen koi* (MPEF-PV 3613), although this condition might be exacerbated in TMM 31100-1334. The width of the frontals at the level of the dorsalmost point of the orbit is about two thirds or more of the maximum width of the skull roof in taxa such as the non-archosaurian archosauromorphs *Teyujagua paradoxa* (Pinheiro et al., 2016) and *Euparkeria capensis* (SAM-PK-5867), the pterosaur *Cacibupteryx caribensis* (cast of IGO-V-208), the herrerasaurid *Herrerasaurus ischigualastensis* (PVSJ 407), and in the sauropodomorphs *Buriolestes schultzi* (CAPP/UFMS 0035) and *Plateosaurus engelhardti* (SMNS 13200; AMNH 6810). The posterior portion of the skull roof of TMM 3110-1334 is dorsally arched, resembling the condition in *I. polesinensis* (ULBRA-PVT059). On the left side of the braincase, the portion of the skull roof anterior to the supratemporal fenestra forms an angle

of  $\sim 30^\circ$  with respect to that formed by the parietal. On the right side, the angle formed between the two surfaces is  $\sim 45^\circ$ , but this is likely exacerbated by some distortion (Figures 2 and 4).

### 3.3 | Frontals

The dorsal surface of the frontals forms the anterior part of the skull roof (Figures 2 and 4), whereas the ventral surface, together with the laterosphenoids more ventrally, forms the roof of the endocranial cavity at the portion corresponding to the olfactory tract. The frontals contact the parietals posteriorly in archosauriforms, but no sign of the suture between these elements is seen in TMM 31100-1334. Also, there is no indication of a supratemporal fossa anterior to the anterior margin of the supratemporal fenestra, which is located at the anterolateral projection of the parietal (see below). Thus, the condition of TMM 31100-1334 is similar to that of the lagerpetid *I. polesinensis* (ULBRA-PVT059), the pterosaur *Allkaruen* (MPEF-PV 3613), the non-archosaurian archosauromorphs *T. paradoxa* (Pinheiro et al., 2016), *E. capensis* (SAM-PK-5867), and *Proterosuchus alexanderi* (Ezcurra & Butler, 2015), and the silesaurid *Silesaurus opolensis* (ZPAL Ab III/361; ZPAL Ab III/362). Differently, early diverging dinosaurs such as *Saturnalia tupiniquim*

**TABLE 1** List of specimens of each comparative taxon used in the present study that were first-hand analyzed by at least one of the authors.

Taxon	Source of information
<i>Allkaruen koi</i>	MPEF-PV 3613
<i>Arizonasaurus babbitti</i>	MSM P459
<i>Buriolestes schultzi</i>	CAPPA/UFSM 0035
<i>Cacibupteryx caribensis</i>	Cast of IGO-V-208; Gasparini, Fernandez & de la Fuente (2004)
<i>Eodromaeus murphy</i>	PVSJ 562
<i>Erythrosuchus africanus</i>	Gower, 1997
<i>Euparkeria capensis</i>	SAM-PK-7696; SAM-PK-5867
<i>Herrerasaurus ischigualastensis</i>	PVSJ 407
<i>Heterodontosaurus tucki</i>	SAM-PK-K337
<i>Ixalerpeton polesinensis</i>	ULBRA-PVT059
<i>Lesothosaurus diagnosticus</i>	NHMUK PV R8501
<i>Lewisuchus admixtus</i>	PULR-V 01
<i>Lagosuchus talampayensis</i>	PVL 3872
<i>Megapnosaurus rhodesiensis</i>	QG 195, QG 197
<i>Panphagia protos</i>	PVSJ 8743
<i>Parringtonia gracilis</i>	NMT RB426
<i>Plateosaurus engelhardti</i>	MB.R.5586-1; SMNS 13200; AMNH 6810
<i>Saturnalia tupiniquim</i>	MCP 3845 PV
<i>Silesaurus opolensis</i>	ZPAL Ab III/361; ZPAL Ab III/362
<i>Sphenosuchus acutus</i>	SAM-PK-K3014
<i>Tawa hallae</i>	GR 241
<i>Triopticus primus</i>	TMM 31100-1030

(MCP-3845-PV) and *H. ischigualastensis* (PVSJ 407) and apparently the pterosaur *Caelestiventus hanseni* (Britt et al., 2018: fig. 3n) exhibit a supratemporal fossa extending anteriorly on the dorsal surface of the frontal (Cabreira et al., 2016). In pseudosuchians, there is also variation of the presence of a supratemporal fossa on the frontals, which is present in taxa such as the crocodylomorphs *Hesperosuchus agilis*, *Sphenosuchus acutus* (SAM-PK-K3014), *Protosuchus richardsoni* and the non-crocodylomorph suchians *Postosuchus kirkpatricki* and *Batrachotomus kupferzellensis* (see Nesbitt, 2011). The anterior portion of the frontals terminates in an interdigitating suture that would have contacted the nasals (Figure 2).

The dorsal surface of the frontals is domed over the orbits where the anterior portion of the frontals extend

anteroventrally. A well-preserved surface bears a light pattern of anastomosing grooves on the right frontal just dorsal to the midline of the orbit. The posterolateral portion of the frontal extend laterally to define an articulation surface defined as an anteriorly opening fossa. Either a postorbital, as in dinosaurs, or a postfrontal, as in *I. polesinensis* (Cabreira et al., 2016), articulated into this facet (Figures 2–4). Anterior to this articulation, there is a laterally extended, dorsoventrally compressed process originating as a ridge on the posterolateral side of the frontal. This process is broken on the left side but more complete on the right side, although the anterior and lateralmost edges appear broken. This lateral process may have served as an articulation facet for the prefrontal, as is the case in *V. gassenae* (Müller et al., 2023).

### 3.4 | Parietals

The parietals of TMM 31100-1334 are completely preserved (Figures 2 and 4). They contact the frontals anteriorly, the postparietal posteromedially, the laterosphenoids anteroventrally, the supraoccipital posteriorly and posteroventrally, and the otoccipital posteroventrally. The anteroposterior length of the parietals, bordering the supratemporal fenestra, is 9.80 mm—the whole length of the parietals was possibly greater than that, but the anterior limit cannot be precisely determined (Figure 2—see dotted suture for approximate location)—and the width of both bones together corresponds to 19.90 mm. Thus, each parietal is approximately as long as wide. This differs from the condition observed in the lagerpetid *I. polesinensis* (ULBRA-PVT059), which has a longer than broad parietal. Such difference in proportions is partially related to the orientation of the posterior half of the parietal wings. In TMM 31100-1334, these are more laterally oriented than in *I. polesinensis*, with the posterior surface of the parietal wings of those forming angles of respectively c. 45° and 30° with the sagittal plane.

The dorsoventral height of the lateral surface of the right parietal of TMM 31100-1334, better preserved than the left element, is 7.90 mm at the posterior limit of the parietal lateral wing (Figures 2–4). Anteriorly, the bone becomes progressively shorter, and at the level of the anterior margin of the supratemporal fenestra it has a height of 3.25 mm. The anteromedial border of the supratemporal fenestra is formed by an anterolateral projection of the parietal. Its posterior surface, which forms the anteromedial corner of the supratemporal fenestra, is dorsoventrally convex, whereas the portion of the parietal forming the lateral border of the supratemporal fenestra is dorsoventrally concave. There is a socket that is here interpreted as the articulation surface with either the



postfrontal or with the postorbital (Figures 2 and 4) on the lateral limit of the anterior projection of the parietal. The dorsal limit of the supratemporal fenestra in the parietal of TMM 31100-1334 is defined by a rim that extends from the base of the parietal lateral wing, posteriorly, until the anterolateral projection of the parietal. Lateral to this short rim, the ventral surfaces of the parietals are depressed in dorsal view.

The right side of the braincase bears a small foramen located at the mid-length of the lateroventral margin of the parietal on a triple junction with the laterosphenoid anteroventrally and the otoccipital posteroventrally (Figure 3). A foramen in this region is also present in the non-archosaurian archosauriform *E. capensis* (Sobral et al., 2016) and in neotheropods (Sampson & Witmer, 2007), corresponding to the passage of the dorsal head vein. According to Sampson and Witmer (2007), the dorsal head vein anastomoses with the middle cerebral vein inside the braincase, on the posterodorsal region of the skull. Differently from the dorsal head vein, which exits the endocranial cavity laterally, the middle cerebral vein in archosaurs exits posteriorly, typically via a foramen located between the parietal and the supraoccipital, as described for neotheropods (Sampson & Witmer, 2007), the non-archosaurian archosauriform *E. capensis* (Sobral et al., 2016), and the pterosaur *A. koi* (Codorníu et al., 2016). The condition is, however, unclear in TMM 31100-1334. On the right side, the contact between the medial margin of the posterior surface of the parietal lateral wing (3.10 mm wide and 8.30 mm high) with the supraoccipital is better preserved than in the left side (Figures 2 and 4). At the dorsal portion of this contact, there is a small gap between the supraoccipital and parietal. This can represent the foramen for the middle cerebral vein, but it might also correspond to an artifact (breakage or poor preservation of this region). On the left side, there is also a gap between the two bones in a similar position, but it might also be an artifact (e.g., breakage). Yet, if these gaps indeed represent the passage of the middle cerebral vein through the occiput, this would be more dorsally located than that described for *E. capensis* (Sobral et al., 2016, fig. 11b). It is worth mentioning, however, that *E. capensis* also seems to exhibit gaps in similar positions of those in TMM 31100-1334. These are located between the structures labeled as supraoccipital ridges by Sobral et al. (2016, fig. 11b) but were interpreted as possible artifacts.

### 3.5 | Postparietal

Based on the CT data, we observe a division between the posterior margin of the parietals and a triangular osseous

element in TMM 31100-1334. This separation may correspond to either a fracture in the parietals or to a suture between the parietals and the postparietal. The latter forms the posterior portion of the skull roof (Figures 2 and 4). It is triangular in dorsal view, but with a slightly rounded anterior margin. Its maximum width is 11.73 mm at its posterior margin, where it contacts the supraoccipital, between the proximal third of the parietal wings. Anteriorly, it tapers until it contacts the medial portion of the posterior margin of the main body of the parietals. A similar morphology is observed for the postparietal of *E. capensis* (SAM-PK-5867). The total antero-posterior length of this element in TMM 31100-1334 is 4 mm. Its dorsal surface bears a marked medial ridge, the center of which is located at the mid-sagittal plane of the skull, alike the ridge on the dorsal surface of the supraoccipital mentioned above. However, even if the supraoccipital ridge extended until the dorsal limit of the bone, it would not be continuous to the ridge on the postparietal.

### 3.6 | Basioccipital

The basioccipital forms the posteromedial portion of the basicranium of TMM 31100-1334 (Figures 2–5). It contacts the parabasisphenoid anteriorly and the otoccipitals laterodorsally. The basioccipital is almost as long as wide (Figure 5); 10.5 mm long from the tip of the occipital condyle to the tip of its inferred anterior limit, and 10.8 mm at its widest portion, located at the level of the basioccipital components of the basitubera (=basioccipital basitubera). The portion of the basioccipital contributing to the occipital condyle is sub-circular in occipital view, with both a maximum height and width of 4.4 mm (Figure 4). However, the whole occipital condyle is wider than high, because the otoccipitals contribute to its dorsolateral corners as in other archosauromorphs. Each otoccipital adds 1.7 mm to the width of the condyle laterally (Figure 4), so that its maximum width is 7.9 mm. A shallow sub-circular pit (1.3 mm in diameter) is located on the dorsal portion of the occipital condyle, in the basioccipital component, between the otoccipital portions of the condyle. This pit is here interpreted as the “notochordal pit” (sensu Gower, 2002), which is also visible in some pseudosuchians (Gower, 2002), some dinosauromorphs (e.g., *Lewisuchus admixtus* [PULR-V 01], *S. tupiniquim* [MCP 3845 PV], *P. engelhardti* [MB.R.5586-1; AMNH 6810], *Tawa hallae* [GR 241]), and is particularly deep in proterochampsians (Ezcurra, 2016). Dorsal to the notochordal pit, CT data show that the dorsal surface of the basioccipital of TMM 31100-1334 extends anteriorly to form part of the floor of the endocranial cavity.

However, possibly the result of poor preservation, the virtually reconstructed dorsal surface of the basioccipital is uneven, revealing not much morphological details for this area. However, it is possible to observe that the dorsal surface of the basioccipital forms the posterior portion of the endocranial cavity between the ventral margins of the otoccipitals, extending anteriorly until the level of the posterior margin of the metotic foramen. Anterior to this point, poor preservation and/or fusion of elements prevents us to determine if the basioccipital separates the left and right otoccipitals, or if these meet medially.

On the ventral surface of the basioccipital, a clear rim circumscribes the anterior limit of the occipital condyle (Figures 5 and 6). The condyle is posteroventrally oriented in lateral view if the main axis of the frontals and parietals is set horizontal, as also seen in the lagerpetid *I. polesinensis* (ULBRA-PVT059) and the pterosaurs *A. koi* (MPEF-PV 3613) and *C. caribensis* (cast of IGO-V-208). A marked protuberance is present approximately at the center of the ventral surface of the basioccipital (Figures 5 and 6), which is absent in *I. polesinensis* (ULBRA-PVT059), *A. koi* (MPEF-PV 3613), and *C. caribensis* (cast of IGO-V-208). This protuberance is identified as a medial component of the basioccipital contribution to the basitubera. A pair of ridges (Figures 5 and 6), one ridge on each side, extends anterolaterally from the medial component, reaching the ventral portion of the parabasisphenoid components of the basitubera (=basisphenoid basitubera). On the better-preserved right side, the ridge forms a ventrally directed lamina, extending 1.5 mm from the ventral surface of the basioccipital body. The pair of ridges forms the posterior limit of the basisphenoid recess (see below) and, together with the parabasisphenoid component of the basitubera, are ventrally offset, at the structure between the two bones, in relation to the ventral surface of the basioccipital. TMM 31000-1334 also has two protuberances on the left and right sides of the ventral surface anterior to the occipital condyle, to this medial element, which are identified as the lateral components of the basioccipital basitubera (see discussion below).

It is not possible, even with the aid of CT data, to determine which bone, that is, basioccipital or parabasisphenoid, forms the ventral margin of the metotic foramen (sensu Gower & Weber, 1998; Figure 6). In specimens with this region visible, for example several dinosaurs (e.g., *S. tupiniquim* [MCP 3845 PV], *P. engelhardti* [MB.R.5586-1], *Efraasia minor* [Bronzati & Rauhut, 2017], *T. hallae* [GR 241]), suchians (e.g., *Parringtonia gracilis* [NMT RB426], *Arizonasaurus babbitti* [MSM P459]), and non-archosaurian archosauriforms (e.g., *E. capensis* [SAM-PK-7696]), the ventral border of the foramen is formed only by the basioccipital.

Regarding the posterior margin of the foramen, it is formed by the otoccipital and basioccipital in TMM 31000-1334. Starting at the foramen, the suture between those two bones extends posteriorly along the lateral surface of the braincase, forming a nearly straight sub horizontal line, until the occipital condyle. We were not able to recognize an unossified gap (sensu Gower & Weber, 1998) in the region of contact among the otoccipital, basioccipital, and parabasisphenoid. Most early dinosauriforms with complete braincases (e.g., *L. admixtus* [PULR-V 01], *Lagosuchus talampayensis* [PVL 3872], *S. tupiniquim* [MCP 3845 PV], *Eodromaeus murphi* [PVSJ 562], *Megapnosaurus rhodesiensis* [QG 195, QG 197]) also lack this gap, whereas it is present in the non-archosaurian archosauriform *E. capensis* (SAM-PK-7696; SAM-PK-5867), and in most non-sauropodan sauropodomorphs, such as *B. schultzi* (CAPPA/UFSM 0035), *P. engelhardti* (MB.R.5586-1; SMNS 13200; AMNH 6810), and *Thecodontosaurus antiquus* (Bronzati & Rauhut, 2017).

With the aid of the CT data, it was possible to determine the anterior limits of the basioccipital, and its contact with the parabasisphenoid on the ventral portion of the braincase, at the region of the basisphenoid recess (Figure 5). TMM 31100-1334 possesses a “U shaped” contact between these elements (see Bronzati & Rauhut, 2017), with the basioccipital projecting anteriorly between the posterolateral portions of the parabasisphenoid, which include the basitubera component. This median projection of the basioccipital has a maximum anteroposterior length of 2.7 mm. Its maximum width, on the surface medial to the basisphenoid basitubera, is 3.1 mm and it becomes slightly narrower anteriorly, ending in a rounded margin. The ventral surface of the anteriorly tapering part of the basioccipital is longitudinally concave and confluent with the basisphenoid recess (sensu Witmer, 1997) on the ventral surface of the parabasisphenoid (Figures 2–6). Because there is no clear division between the recess in the basisphenoid and in the basioccipital, we here consider that the basisphenoid recess of TMM 31100-1334 also continues onto the latter bone (Figures 5 and 6). This configuration is similar to that of the dinosaurs *M. rhodesiensis* (QG 195, QG 197), *E. minor* (Bronzati & Rauhut, 2017), and *B. schultzi* (CAPPA/UFSM 0035), the pterosaurs *A. koi* (MPEF-PV 3613) and *C. caribensis* (cast of IGO-V-208), and the suchian *P. gracilis* (NMT RB426). On the other hand, the recess seems to be restricted to the parabasisphenoid in taxa such as the non-archosauriform diapsid *Youngina capensis* (Gardner et al., 2010, fig. 5) and the non-archosaurian archosauriforms *Azendohsaurus madagaskarensis* (UA 7-20-99-653). Note that here we are homologising the depression on the ventral surface of the braincase of the above mentioned taxa, regardless of its extension to the basioccipital, to the basisphenoid recess of Witmer (1997).

An additional blind pit (Figure 5) is present within the basi-sphenoid recess of the basioccipital of TMM 31100-1334. Blind pits on the ventral surface of the basioccipital are common in dinosauromorphs (Bronzati et al., 2019) and also present in some pseudosuchians (Nesbitt, 2011), but with variation across taxa regarding the number of pits. A single blind pit as in TMM 31100-1334 is also observed in the lagerpetid *I. polesinensis* (ULBRA-PVT059) and the dinosauromorphs *L. admixtus* (PULR-V 01), *S. opolensis* (ZPAL Ab III/361; ZPAL Ab III/362), and *B. schultzi* (CAPP/UFMS 0035). Other archosaur taxa such as the neotheropod *M. rhodesiensis* (QG 195, QG 197) and the suchian *S. acutus* (SAM-PK-K3014) exhibit a pair of pits divided by a median ridge on the midline.

### 3.7 | Parabasisphenoid

The parasphenoid (dermal ossification) and the basisphenoid (endochondral ossification) are typically fused in post-hatchling sauropsids (Sampson & Witmer, 2007). In archosaurs, the “parasphenoid portion” of the parabasisphenoid is typically restricted to the cultriform process, but this structure is not entirely preserved in TMM 31100-1334 (Figures 3–6). Nevertheless, we adopt the term parabasisphenoid (sensu Gower & Weber, 1998) to refer to the element formed by the fusion of the parasphenoid and basisphenoid (e.g., Bronzati & Rauhut, 2017; Sampson & Witmer, 2007), even if only the “basisphenoid portion” of the parabasisphenoid is preserved.

The preserved anteroposterior length of the parabasisphenoid is 11.25 mm, and its maximal lateromedial width, measured at the level of the basitubera (Figure 5), is 10.25 mm. However, anterior to the basitubera, the ventral surface of the parabasisphenoid rapidly tapers to a width of 6.1 mm at the level of the basiptyergoid processes. A depression extends for almost the entire ventral surface of the bone, which is here interpreted as the basisphenoid recess (Figure 5). Previous workers have used the term median pharyngeal recess to refer to this depression (Nesbitt, 2011; Nesbitt et al., 2018; Sobral et al., 2016), but following the discussion by Bronzati et al. (2019), we employ the term basisphenoid recess as originally proposed by Witmer (1997). As mentioned above, the posterior limit of the basisphenoid recess expands onto the basioccipital, whereas its anterior limit is defined by a rim located at the posterior edge of the base of the basiptyergoid processes (not completely preserved in TMM 31100-1334). The basisphenoid recess is deeper at the center of the parabasisphenoid ventral surface, becoming progressively shallower anteriorly and toward its lateral margins. The recess lacks a sharply

defined lateral rim, but a sharp angle marks the transition between the ventral and lateral surface of the parabasisphenoid (Figures 5 and 6). This angle marks the ventral boundary of the anterior tympanic recess on the lateral wall of the braincase, extending from the most anterior edge of the preserved portion of the parabasisphenoid to its component of the basitubera. A basisphenoid recess was observed in all taxa analyzed for this study (Table 1).

The description of the parabasisphenoid components of the basitubera of TMM 31100-1334 is based on the left element, which it is more completely preserved (Figures 5 and 6). We interpret the left parabasisphenoid basitubera as an anteroposteriorly compressed lamina, nearly 4.35 mm high dorsoventrally. It is located at the posterolateral corner of the ventral surface of the parabasisphenoid. Circular pits and grooves (i.e., muscle scars), related to craniocervical musculature (Snively & Russell, 2007), are scattered across this region of the parabasisphenoid surface. The posterolateral limit of the parabasisphenoid basitubera is separated from the lateral component of the basioccipital basitubera by a groove, indicating that these represent separate attachment sites for the craniocervical musculature, that could be associated with different muscles (e.g., *M. rectus capitis ventralis*, *M. longissimus capitis*—Snively & Russell, 2007).

The dorsal limit of the parabasisphenoid cannot be recognized in the lateral wall of the braincase of TMM 31100-1334, even with CT data. Consequently, our description of such lateral surface focuses on the shape of the excavation located in this region, which is here interpreted as the anterior tympanic recess (sensu Witmer, 1997). The recess is better preserved and more visible on the right side of the braincase, whereas on the left side figures and part of the prootic is medially folded, covering the dorsal portion of the recess (Figures 3 and 6). Thus, our description is based on the right side of the specimen. As mentioned above, the portion that corresponds to the transition between the ventral and lateral surfaces of the parabasisphenoid delimits the anterior tympanic recess ventrally. The posterior limit of this recess is marked by a pillar of bone (triangular in lateral view) dorsal to the parabasisphenoid component of the basitubera, which is dorsally confluent with the ventral ramus of the otosphenoidal crest sensu Sampson and Witmer (2007) (Figures 3 and 6). The dorsal portion of the recess invades the lateral surface of the prootic near the foramen for the facial nerve (VII—see below). In this case, this dorsal portion could be equivalent to a subdivision of the anterior tympanic recess, i.e., the prootic recess, as in neotheropods (Witmer, 1997). The maximal extension (from the posterodorsal to the anteroventral corner) of the anterior tympanic recess (including its



prootic part) is of nearly 10 mm. In *A. koi* (MPEF-PV 3613), the lateral surface of the parabasisphenoid is invaded by two depressions, interpreted as the anterior tympanic recess and the basiptyergoid recess (Codorníu et al., 2016). These two recesses are topologically equivalent to the anterior tympanic recess of TMM 31100-1334, suggesting that the development of a basiptyergoid recess in *A. koi* (MPEF-PV 3613) could result from the subdivision of the plesiomorphic anterior tympanic recess.

The surface within the anterior tympanic recess of TMM 31100-1334, ventral to the foramen for the exit of cranial nerve VII, bears a series of pits (Figures 3 and 6), similar to the pockets described for the theropod *Piatnitzkysaurus floresi* as pneumatic in origin (Rauhut, 2004). Additionally, a depression at the anteroventral corner of the recess likely corresponds to the lateral opening associated with the entrance of the internal carotid artery. In most dinosauromorphs, the internal carotid artery enters the endocranial cavity through an aperture in this region (Nesbitt, 2011). One exception is *S. opolensis* (ZPAL Ab III/361; ZPAL Ab III/362), in which the passage of the internal carotid artery is on the ventral surface of the parabasisphenoid, as in most stem-archosaurs and some pseudosuchians (Nesbitt, 2011). However, neither condition can be confirmed for TMM 31100-1334, even with the aid of the CT data, because no clear connection between this depression and the hypophyseal fossa (see below) can be identified. Anteriorly, the anterior tympanic recess is roofed by the otosphenoidal crest (Figures 3 and 6). Medial to the crest, the anterior surface the parabasisphenoid is 2.30 mm wide (transversely), extending till the lateral limit of the hypophyseal fossa, but no details of this structure can be recognized in TMM 31100-1334. The hypophyseal fossa would have housed the pituitary gland, based on comparisons with living crocodylians and birds, and thus inferred as present in extinct archosaurs (Witmer et al., 2008). The parabasisphenoid contacts the prootic dorsally in the region of attachment for *M. protractor pterygoideus* (see below).

### 3.8 | Prootic

Left and right prootics of TMM 31100-1334 are preserved and have their lateral surface exposed, whereas some aspects of their medial surface can be accessed with the CT data (see below). The left element (Figures 3 and 6) is broken and folded medially at the dorsoventral level of the foramen for the cranial nerve V (trigeminal). The right element preserved some structures typically associated with the prootic that cannot be seen on the left side, such as the foramen for the exit cranial nerve VII (facial), an additional foramen dorsal to the foramen for the exit of cranial nerve V (trigeminal; see below), and a preotic

pendant (Figures 3 and 6). As a result, we provide here the description of the TMM 31100-1334 prootic based on the right element. It is worth mentioning that we cannot recognize any noteworthy difference between the preserved parts of the left and right elements.

A small but distinct protuberance (Figures 3 and 6) on the ventrolateral surface of the prootic, located 2.65 mm posteroventral to the notch associated to the trigeminal nerve, is here interpreted as the preotic pendant (Figure 6) sensu Sampson and Witmer (2007). The preotic pendant is a surface for the anchorage of masticatory muscles such as the *M. protractor pterygoideus* and *M. levator pterygoideus* (Holliday, 2009), and it has also been treated as the *ala basisphenoidalis* (Chure & Madssen, 1996), because it is formed by the basisphenoid in some taxa. Yet, as discussed previously (e.g., Bronzati & Rauhut, 2017; Sampson & Witmer, 2007), this structure is sometimes composed of both the prootic and the basisphenoid. As in *D. gregorii*, the preotic pendant is “poorly developed,” i.e. not covering part of the anterior tympanic recess as in non-avian theropods (Rauhut, 2004; Sampson & Witmer, 2007).

The foramen for the trigeminal nerve of TMM 31100-1334 is completely enclosed within the prootic (Figures 3 and 6), as in *I. polesinensis* (ULBRA-PVT059). Our interpretation is that the trigeminal ganglion (sensu George & Holliday, 2013) would seat in a surface adjacent to the ventral part of this foramen, where a shallow depression is observed on the lateral surface of the prootic. The narrower dorsal portion of the foramen likely corresponds to the path for the ophthalmic nerve (V1, the first branch of the trigeminal ganglion). This interpretation is also based on the presence of a groove that extends onto the lateral surface of the laterosphenoid.

An additional foramen is located anterodorsal to the foramen for the passage of trigeminal nerve (Figure 3). A groove is associated to this foramen and extends posteroventrally for 2.05 mm until the same horizontal level of the otosphenoidal crest (see below) and then bows to assume a posterodorsal orientation. This path is similar to that of the middle cerebral vein of, for example, theropods (Sampson & Witmer, 2007), so that the foramen is here interpreted as associated with that vein rather than with the ophthalmic nerve, which, when present, is typically more anteriorly located (Holliday, 2009; Sampson & Witmer, 2007). The exits of the middle cerebral vein and the trigeminal nerve from the endocranial cavity varies greatly among archosaurs (e.g., Bronzati & Rauhut, 2017; Nesbitt, 2011; Rauhut, 2003; Sampson & Witmer, 2007). The presence of separate openings, as in TMM 31100-1334, is observed among some neotheropods (Rauhut, 2003; Sampson & Witmer, 2007) and in pseudosuchians such as *Stagonolepis robertsoni* (Walker, 1990),

*Desmatosuchus spurensis* (Small, 2002), and *Longosuchus meadei* (Nesbitt, 2011). In dinosauromorphs such as the silesaurid *S. opolensis* (ZPAL Ab III/361; ZPAL Ab III/362) and the saurischians *T. hallae* (GR 241) and *S. tupiniquim* (MCP 3845 PV), there is no evidence of an additional foramen, so that the middle cerebral vein and trigeminal nerve possibly exited the endocranial cavity through the elongated same foramen. A third condition, observed in sauropodomorphs such as *P. engelhardti* (MB.R.5586-1; AMNH 6810) and *E. minor* (Bronzati & Rauhut, 2017) and in suchians such as *B. kupferzellensis* (Gower, 2002) and *S. acutus* (SAM-PK-K3014), is the presence of bony prongs that subdivide the foramen on the lateral surface of the prootic, but no independent foramina are formed.

We here use the term otosphenoidal crest sensu Sampson and Witmer (2007) to refer to the crest extending on the lateral surface of the braincase of TMM 31100-1334, from the base of the paroccipital process, posteriorly, to the basisphenoid, anteriorly (Figures 3 and 6). This is equivalent to the crista prootica of some authors—e.g., Gower and Nesbitt (2006) for the pseudosuchian *Arizonasaurus babbitti* (MSM P459); Martinez et al. (2012) for the sauropodomorph *Panphagia protos*; character 254 of the data matrix of Ezcurra (2016)—and also to the “generically labeled” crests 1 and 2 of *E. capensis* by Sobral et al. (2016)—see Sobral and Müller (2019) for further details on this matter. We here prefer to adopt the term otosphenoidal crest instead of crista prootica, because, as already mentioned by Sampson and Witmer (2007), the crest is not limited to the prootic in some taxa. In some sauropod dinosaurs, the otosphenoidal crest partially covers the fenestra vestibuli (=fenestra ovalis) in lateral view (Tschopp et al., 2015). However, in other dinosauromorphs, the crest is usually configured as a low ridge without a significant lateral expression, as is the case in TMM 31100-1334. Our interpretation is that the otosphenoidal crest in TMM 31100-1334 extends posteriorly until the paroccipital process because of the presence of a ventral keel (Figure 3) that creates a step between the area of the stapedial groove (dorsal to the fenestra vestibuli) and the laterodorsal surface of the otoccipital and prootic. Anteriorly, the otosphenoidal crest is more evident at the anteroposterior level of the recess associated to the foramen for cranial nerve VII (facial), where the crest bifurcates (Figures 3 and 6). The anterior component extends anteroventrally, forming the anterior margin of the recess where the foramen for the facial nerve is located and becomes confluent with the prootic pendant described above. The posterior component delimits the posterior border of the facial nerve recess. Ventrally, it becomes thicker, marking the posterodorsal limit of the anterior tympanic recess (i.e., the pillar of bone mentioned above).

The facial nerve has two distinct rami, the hyomandibular and the palatine (Holliday, 2009), and two grooves adjacent to the foramen likely represent the distinct paths of each ramus on the lateral surface of the braincase of TMM 31100-1334. One of these grooves extends posterodorsally, between the two components of the division of the otosphenoidal crest mentioned above (Figures 3 and 6). This is consistent with the path of the hyomandibular ramus of the nerve as described for dinosaurs (Galton, 1985; Holliday, 2009), which after leaving the endocranial cavity turns posteriorly, toward the dorsolateral surface of the paroccipital process. The second groove extends anteriorly, on the dorsal surface of the ridge corresponding to the posterodorsal limit of the anterior tympanic recess (Figures 3 and 6). At the anterior limit of this ridge, the groove assumes an anteroventral orientation, leaving a mark on the ridge and entering the space of the anterior tympanic recess. This path is consistent with that of the palatine ramus of the facial nerve of dinosaurs (Holliday, 2009). Bronzati and Rauhut (2017), following Galton (1985), mentioned that the palatine ramus of the facial nerve in sauropodomorphs passes through the foramen for the internal carotid artery, located within the anterior tympanic recess. This is, however, an unlikely scenario in cases where the lateral aperture for the internal carotid artery in the anterior tympanic recess is narrow (Holliday, 2009), likely the case of TMM 31100-1334. Thus, the most plausible scenario is that the palatine ramus would exit the anterior tympanic recess laterally and then turn ventrally in the region of the basiptyergoid process of TMM 31100-1334, as described for some dinosaurs (Holliday, 2009). This is also likely the case for taxa that do not exhibit a foramen for the internal carotid artery within the lateral surface of the parabasisphenoid, as is the case in non-archosaurian archosauriforms, *S. opolensis* (ZPAL Ab III/361; ZPAL Ab III/362), and some early pseudosuchians (Nesbitt, 2011).

The medial surface of the prootic can be accessed with the CT data, but as for the other bones, the reconstructed medial surface is uneven as a result of post burial compression during fossilization. The only recognizable structure is a large floccular fossa, which likely housed some of the soft tissues of the cerebellum, including the flocculus and the paraflocculus (Walsh et al., 2013). The floccular fossa of TMM 31100-1334 is 4.70 mm deep and cone-shaped, with a higher diameter (3.50 mm) proximally (where the fossa is connected to the rest of the endocranial cavity), and tapering distally.

### 3.9 | Otoccipital

We use the term otoccipital here to refer to the element formed by the fusion of the opisthotic and exoccipital (sensu Sampson & Witmer, 2007), located on the

posterodorsal region of the braincase (Figures 2–4 and 6). Structures typically associated with the otoccipital (solely or partially) that are present in TMM 31100-1334 consist of the dorsolateral corners of the occipital condyle, the foramen magnum (see description of the basioccipital above), the foramina for cranial nerve XII (hypoglossal), the metotic foramen, the fenestra vestibuli, and the dorsal tympanic recess.

The posterolateral projection of the otoccipitals corresponds to the paroccipital process, but only the base of this structure is preserved in TMM 31100-1334 (Figures 2–4 and 6). Thus, not much detail (e.g., orientation, length) can be provided. The lateral surface of the bone is dorsoventrally concave, between the otosphenoidal crest ventrally and the contact with the parietal dorsally. The dorsoventral height of this portion of the bone is 8.10 mm, whereas its anteroposterior extension corresponds to 6.30 mm. These measurements were taken on the right side, as the surface is not entirely visible on the left side, as the result of the ventral displacement of the parietals. The most distinguishing feature of this region, as seen on the right side, is a circular depression (Figure 3), with a diameter of 2.65 mm. On the left side, a depression is also present, but not with so well-marked limits. As discussed by Witmer (1997), a dorsal tympanic recess is usually present in the prootic of early archosaurs, at the portion of this bone that overlaps the otoccipital, with the recess sometimes extending posteriorly onto the otoccipital and onto the laterosphenoid anterodorsally. A depression on this region is common among dinosauromorphs (Bronzati et al., 2019). Additionally, a depression is also observed in the non-archosaurian archosauriform *E. capensis* (SAM-PK-7696), and in pseudosuchians such as *P. gracilis* (NMT RB426) and *Arizonasaurus babbitti* (MSM P459). This could indicate that the dorsal tympanic recess is also widespread among pseudosuchian archosaurs. It seems however that the depression of TMM 31100-1334 is more posteriorly located than the dorsal tympanic recess of the taxa mentioned above. In TMM 31100-1334, the depressions on both sides of the braincase do not extend anteriorly until the level of the foramen for the facial nerve. In the other above taxa, the anterior and/or dorsal limits of the recess are not always evident, although the recess usually extends anteriorly beyond the horizontal level of the foramen for the facial nerve.

Here we adopt the term exoccipital pillar (sensu Gower, 2002) to refer to the portion of the otoccipitals that forms part of the occipital condyle, and where other structures such as the foramina for the hypoglossal nerve and the posterior margin of the metotic foramen are located (Figures 2–4 and 6). The exoccipital pillar of TMM 31100-1334 is dorsolaterally to ventromedially

oriented in occipital view, forming an obtuse angle to one another (Figures 2–4 and 6). Such non-vertically oriented exoccipital pillars could result from a taphonomic dorsoventral compression of the braincase, but this seems to not be the case because a near-identical condition also occurs in other early avemetatarsalians, such as *I. polesinensis* (ULBRA-PVT059), *L. admixtus* (PULR-V 01), *A. koi* (MPEF-PV 3613), and *C. caribensis* (cast of IGO-V-208). The ventral ends of the exoccipitals do not medially contact one another on the floor of the endocranial cavity, closely resembling the condition in *I. polesinensis* (ULBRA-PVT059) and *A. koi* (MPEF-PV 3613). As typical of archosaurs (Gower, 2002; Sampson & Witmer, 2007; Sobral et al., 2016), TMM 31100-1334 possesses two foramina for the hypoglossal nerve (cranial nerve XII) on each side of the braincase (Figure 6). By contrast, there is a single hypoglossal foramen in the pterosaur *A. koi* (MPEF-PV 3613). On the left side, where this region is completely preserved, a 1.10 mm long and 2.05 mm wide surface separates the posterior hypoglossal foramen from the foramen magnum. As observed among other archosauriforms (Table 1), the posterior of the hypoglossal foramina of TMM 31100-1334 has a greater diameter than the anterior. With the occipital condyle horizontally aligned, the ventral margin of the posterior foramen lies approximately at the same level of the dorsal margin of the anterior one. Dorsal to the openings for the hypoglossal foramina in TMM 31100-1334, a depression is observed on the posterior surface of the lamina (see below) that marks the posterior border of the metotic foramen. However, no additional foramen is visible in this region, similar to what is observed in the non-archosaurian archosauriform *E. capensis* (SAM-PK-7696). Taxa such as the non-dinosaurian dinosauromorph *L. admixtus* (PULR-V 01), and most theropods (Rauhut, 2003) and non-sauropodan sauropodomorphs (Bronzati & Rauhut, 2017) exhibit an additional foramen in this region, an aperture associated with cranial nerve X, the vagus nerve (sensu Gower & Weber, 1998). The absence of this foramen in TMM 31100-1334 indicates that it does not possess a divided metotic foramen (Bronzati & Rauhut, 2017; Gower & Weber, 1998; Sampson & Witmer, 2007).

In TMM 31100-1334, the anterolateral limit of the exoccipital pillar is configured as a mediolaterally expanded lamina, anteroposteriorly compressed, that marks the separation between the anterior foramina for the hypoglossal nerve and the metotic foramen (Figure 6). This lamina extends ventrally until the contact with the basioccipital. Although laterally expanded, this lamina is less laterally projected than the descending ramus of the opisthotic (see below), which forms the anterior and posterior margins of the metotic foramen



and fenestra vestibuli, respectively. This is similar to the condition observed in taxa such as the non-archosaurian archosauriform *E. capensis* (SAM-PK-7696), the pterosaurs *A. koi* (MPEF-PV 3613) and *C. caribensis* (cast of IGO-V-208), the silesaurid *S. opolensis* (ZPAL Ab III/361; ZPAL Ab III/362), and in the saurischians *H. ischigualastensis* (PVSJ 407), *T. hallae* (GR 241), *S. tupiniquim* (MCP 3845 PV), and *P. engelhardti* (MB. R.5586-1; SMNS 13200; AMNH 6810). The opposite condition, i.e., the descending ramus of the opisthotic not extending more laterally than the exoccipital pillar, is observed in theropods such as *M. rhodesiensis* (QG 195, QG 197) and possibly the non-dinosaurian dinosauriform *L. admixtus* (see Nesbitt, 2011).

On the left side of the braincase of TMM 31100-1334, where the descending ramus of the opisthotic (sometimes termed as crista interfenestralis—see Sampson & Witmer, 2007) is better preserved, the ramus corresponds to a mediolaterally expanded lamina, anteroposteriorly compressed (0.70 mm in anteroposterior length), and with an estimate width of 4.00 mm (Figures 2–4 and 6). On the right side, a depression on the surface of the otoccipital, posterodorsal to the fenestra vestibuli, and medial and ventral to the otosphenoidal crest, is interpreted as the stapedial groove (Figures 3–6). Finally, more details on the size of the apertures related to the metotic foramen and fenestra vestibuli are hampered by the poor preservation of the ventral rami of the paroccipital process delimiting both structures on both sides of the braincase.

### 3.10 | Laterosphenoid

Here we use the term laterosphenoid to refer to the osseous element of TMM 31100-1334 that contacts the ventral surface of the frontal anteriorly, until the level of the foramen for the trigeminal nerve posteroventrally, and the foramen for the dorsal head vein posterodorsally (but see discussion below). Our description is based on the right element (Figures 3 and 7), which is better preserved and shows a congruent shape in relation to its counterpart.

The posterodorsal limit of the laterosphenoid forms, together with the parietal and the otoccipital, the border of a foramen interpreted here as the passage for the dorsal head vein. Anterior to this foramen, the dorsal margin of the laterosphenoid contacts the parietal until the level of a lateral projection that curves posteriorly at its tip, which corresponds to the capitata process (Figures 3 and 7). The bone is slightly medially displaced in this region and, in the original position, the capitata process would likely be located ventral to an anterolateral projection of the parietal that forms the anteromedial corner of the

supratemporal fenestra. The lateral surface of the laterosphenoid, between the foramen for the dorsal head vein and the capitata process is anteroposteriorly concave, following the shape of the lateral margin of the parietal at the border of the supratemporal fenestra. Ventrally, the laterosphenoid contacts the prootic.

A groove that extends from the dorsal margin of the trigeminal foramen until the base of the capitata process of the laterosphenoid, represents the path of the ophthalmic branch of the trigeminal nerve. A similar groove is clearly visible in taxa such as the non-archosaurian archosauriforms *E. capensis* (Sobral et al., 2016, fig. 15), *Erythrosuchus africanus* (Gower, 1997, fig. 6b), and *P. alexanderi* (Clark et al., 1993, fig. 2). On the other hand, the groove is lacking in taxa such as the ornithomirans *A. koi* (MPEF-PV 3613), *S. tupiniquim* (MCP 3845 PV; Bronzati et al., 2019, fig. 2), and *T. hallae* (GR 241), or it is at least not as evident as in the other taxa mentioned above. Dorsally, the groove in TMM 31100-1334 is delimited by a low crest that extends onto the surface of the capitata process, dorsally, until almost the contact with the prootic, ventrally. We interpret this crest as homologous to the cotylar crest of Holliday and Witmer (2009), but not to the cotylar crest of Clark et al. (1993). As described by Holliday and Witmer (2009), following Busbey (1989), this crest represents the attachment site for muscle *M. adductor mandibulae externus profundus* in extant crocodylians.

The anterior limit of the groove associated to the ophthalmic branch of the trigeminal nerve is marked by a sharp ridge (Figures 3 and 7) in TMM 31100-1334. A topologically equivalent structure was identified as the cotylar crest in *P. alexanderi* by Clark et al. (1993). However, we follow Holliday & Witmer (2009; p. 719) and interpret this ridge as the laterosphenoid buttress, which separates the orbital (anterior) and temporal (posterior) surfaces of the laterosphenoid—Sobral et al. (2016) also interpreted this structure as the laterosphenoid buttress in the non-archosaurian archosauriform *E. capensis*. In TMM 31100-1334, a concave surface is formed between the dorsal limit of the laterosphenoid buttress and the base of the capitata process. This surface is continuous with the groove associated with the ophthalmic branch of the trigeminal nerve described above and might represent the point of entrance of this branch of the nerve into the orbital region.

In TMM 31100-1334, a foramen (Figures 3 and 7) is located 2.31 mm anteromedial to the dorsal limit of the laterosphenoid buttress, at the same dorsoventral level of the base of the capitata process. This is a small foramen, 1.00 mm in diameter, but it is clearly present in both laterosphenoids. We interpret this foramen as the opening for cranial nerve IV (trochlear), as identified by Gower (1997) for *E. africanus*. However, this differs from

the interpretation of Clark et al. (1993) for *P. alexanderi*, in which a topologically equivalent foramen was identified as the passage for the ophthalmic artery. Ventral and slightly posteriorly to the foramen interpreted here as that for the trochlear nerve, and anterior to the foramen for the trigeminal nerve, it is possible to observe another opening in the laterosphenoid of TMM 31100-1334. This opening can represent the foramen for cranial nerve III (oculomotor), a position that is consistent with that of the oculomotor nerve as described for *E. capensis* (Sobral et al., 2016) and *E. africanus* (Gower, 1997)—that is, anterior and at the same dorsoventral level of the trigeminal foramen, anterior to the anterior margin of the laterosphenoid buttress, and ventral to the opening for the trochlear nerve. The foramen for the oculomotor nerve is also present in an equivalent position in dinosaurs, but with a much larger aperture (see e.g., Bronzati et al., 2019; Bronzati & Rauhut, 2017; Chappelle & Choiniere, 2018; Sampson & Witmer, 2007). Finally, it is worth mentioning that an aperture dorsal to that associated here to the oculomotor nerve is present in the right laterosphenoid of TMM 31100-1334. However, this is interpreted as a breakage, rather than a passage associated to soft tissues, because it is continuous with a line of fracture.

The ventral portion of the right laterosphenoid of TMM 31100-1334 is preserved underneath the ventral portion of its counterpart (Figure 7). Anterior to the laterosphenoid buttress, the laterosphenoid forms a triangular lamina, with a straight dorsal margin. This dorsal margin marks the contact of the bone with the ventral surface of the frontal. The dorsoventral height of this lamina, at the level of the opening for the trochlear nerve, is 12.00 mm, and the surface becomes progressively shallower anteriorly, reaching its anterior preserved limit with a height of 4.75 mm. The lateral surface of this region of the laterosphenoid is dorsoventrally convex, whereas the medial surface is concave, surrounding the olfactory tract together with the frontals dorsally.

### 3.11 | Supraoccipital

The supraoccipital of TMM 31100-1334 is completely preserved, although with some breakage and distortion (Figures 2 and 4). As preserved, the maximum width of the bone is 16.20 mm, at the level of its contact with the otoccipital at the margin of the posttemporal fenestra. The maximum height of the bone is 13.4–14.5 mm, taking into account the uncertainty regarding its ventral limit. Despite the distortion, the supraoccipital is wider than high, which is the typical condition among early ornithodirans (e.g., *I. polesinensis* [ULBRA-PVT059]; *H. ischigualastensis* [PVSJ 407], *T. Hallae* [GR 241],

*Panphagia protos* [PVSJ 8743]) and also seen in the non-archosaurian archosauriform *E. capensis* (SAM-PK-7696; SAM-PK-5867). The Early Jurassic ornithischians *Heterodontosaurus tucki* (SAM-PK-K337) and *Lesothosaurus diagnosticus* (NHMUK PV R8501) have a supraoccipital higher than wide (Porro et al., 2015). The contribution of the supraoccipital to the border of the foramen magnum is unclear in TMM 31100-1334 (Figures 2 and 4). It is possible to trace its suture with the otoccipital, with the ventrolateral corners of the former sitting over the bases of the paroccipital processes of the latter. However, the suture between these bones at the level of the foramen magnum is not clear.

The supraoccipital forms the lateral border of the posttemporal fenestra of TMM 31100-1334 (Figures 2 and 4), as in the non-archosaurian archosauriform *E. capensis* (SAM-PK-7696; SAM-PK-5867), the lagerpetid *I. polesinensis* (ULBRA-PVT059), and possibly the pterosaur *A. koi* (MPEF-PV 3613); note that based on its equivalent position with the posttemporal fenestra of other archosauriforms, we consider that the medial opening on the occiput of the latter species corresponds to the posttemporal fenestra rather than to the exit of the caudomedial vein, as suggested by Codorniu et al. (2016). The ventral border of that fenestra in TMM 31100-1334 is formed by the paroccipital process of the otoccipital, whereas the dorsal border is formed by the parietal wings. The size of the posttemporal fenestra varies among archosauriforms (Nesbitt, 2011). In *E. capensis* (SAM-PK-5867), its lateromedial width is about the same as that of the foramen magnum. On the other hand, in taxa such as the crocodylomorph *S. acutus* (SAM-PK-K3014) and the pterosaur *A. koi* (MPEF-PV 3613), the lateromedial width of the fenestra is about half the diameter of the foramen magnum. The situation is unclear in TMM 31100-1334, because it lacks the squamosals, which would have formed the lateral border of the posttemporal fenestra, and the paroccipital processes are not completely preserved. Nevertheless, it is safe to state that the fenestra of TMM 31100-1334, as in *I. polesinensis* (ULBRA-PVT059), is larger than that of dinosaurs. Dinosaurs typically have a relatively reduced foramen (e.g., Nesbitt, 2011; Sereno & Novas, 1994) or even no opening at all in this area of the braincase (Sereno & Novas, 1994).

Dorsomedial to the posttemporal fenestra, the supraoccipital of TMM 31100-1334 exhibits a semi-circle shape in posterodorsal view (Figures 2 and 4). The CT data revealed that part of the dorsal margin of the supraoccipital is not preserved. A midline ridge (=nuchal crest) is present on the outer surface of the supraoccipital, more marked on the posteroventral part of the bone (Figures 2 and 4). A 4.15 mm lateromedial width is nearly constant along its preserved extension. Its ventral end reaches the dorsal margin of the foramen magnum, but its dorsal limit is not preserved. In the lagerpetid *I. polesinensis*

(ULBRA-PVT059), the dinosauriform *L. admixtus* (PULR-V 01), and the non-archosaurian archosauriform *E. capensis* (SAM-PK-5867), there is an additional supraoccipital ridge located lateral to the midline ridge, one on each side of the bone. Differently, TMM 31100-1334 lacks these lateral ridges, as also observed in the silesaurid *S. opolensis* (ZPAL Ab III/361; ZPAL Ab III/362) and dinosaurs such as *H. ischigualastensis* (PVSJ 407), *S. tupiniquim* (MCP 3845 PV), *Panphagia protos* (PVSJ 8743), *H. tucki* (SAM-PK-K337), and *L. diagnosticus* (NHMUK PV R8501). The Jurassic pterosaurs *A. koi* (MPEF-PV 3613) and *C. caribensis* (cast of IGO-V-208) have a transversely concave supraoccipital, with a depressed rather than ridged medial region of the bone.

### 3.12 | Brain

The density differences between bones and matrix allowed a reliable rendering of the cranial endocast (Figure 8), especially of the brain, but the exact position and path of some cranial nerves and blood vessels were difficult to determine with certainty. The distortion in the architecture of the braincase mentioned above have an impact on the preservation of the endocranial cavity. Most of the left side of the reconstructed endocast, at the level of the cerebral hemisphere and cerebellum, seems to be collapsed medially. Hence, the description of this region is solely based on the right side.

The pontine flexure, corresponding to the angle formed between the anteroposterior axis of the posterior region of the hindbrain (medulla oblongata) and the oblique axis of the midbrain, at the level of the cerebellum, is of 140°. This is greater than that observed in *I. polesinensis* (ULBRA-PVT059), which is around 125°. Thus, in lateral view, the posterior portion of the hindbrain of TMM 31100-1334 is slightly less flexed than that of *I. polesinensis*. The floccular lobe of the cerebellum projects posterodorsally and invades the space between the semicircular canals (Figure 8). Its dorsoventral height at the base accounts for ~045% of the dorsoventral height of the brain endocast in this region. This is similar to the condition of *I. polesinensis* (ULBRA-PVT059) and the pterosaur *A. koi* (MPEF-PV 3613). On the other hand, the base of the floccular lobe of the cerebellum of other archosaurs is relatively shorter dorsoventrally (Ezcurra et al., 2020). The conical shape of the floccular lobe of TMM 31100-1334 is mostly similar to that of the lagerpetid *I. polesinensis* (ULBRA-PVT059); differing from the more dome-shaped shape of the fossa observed in taxa such as the pterosaur *A. koi* (Codorniu et al., 2016), the dinosauromorphs *L. admixtus* (PULR-V 01), *B. schultzi* (Müller et al., 2020), and *S. tupiniquim* (Bronzati

et al., 2017), and the non-archosaurian archosauriform *Triopticus primus* (Stocker et al., 2016). Anterodorsal to the flocculus or the cerebellum, it is possible to distinguish a protuberance at the dorsal limit of the endocast. This likely represents the dural expansion, a space occupied by the longitudinal venous sinus that is not part of the brain itself (Witmer et al., 2008). As a result of this expansion, the dorsal margin of the endocast anterior to this structure slopes anteroventrally. The right side of the endocast exhibits a lateral expansion at the region of the cerebral hemisphere. Nevertheless, it is difficult to confirm if this corresponds to the original shape of the brain or if it is an artifact caused by the displacement of the left side of the braincase. Finally, it is not possible to distinguish the regions of the endocast corresponding to the olfactory tract and bulb. Nevertheless, the anteroposterior length of these two structures together would account for around one third of the total anteroposterior length of the endocast.

### 3.13 | Endosseous labyrinth

The endosseous labyrinth was reconstructed on both sides of the braincase of TMM 31100-1334 (Figure 8). As previously reported, the semicircular canals of TMM 31100-1334 are relatively large in comparison with other archosaurs, with a size that approaches that observed in non-avian dinosaurs and living birds (Bronzati et al., 2021). Its anterior semicircular canal (ASC) is the longest, approximately two times longer than the lateral (LSC) and posterior (PSC) canals (ASC = 14.92/14.14 mm; LSC = 6.74/6.31 mm; PSC = 7.05/6.88 mm; common crus = 2.77/2.80 mm; values correspond to the left and right sides, respectively). In lateral view, the ASC assumes the shape of an arch, a result of its great degree of circularity. This condition is also observed in *I. polesinensis* (ULBRA-PVT059), and in pterosaurs, including *A. koi* (MPEF-PV 3613), in stem-archosaurs such as *T. primus* (TMM 31100-1030) and *Trilophosaurus buettneri* (Bronzati et al., 2021), and also in some non-avian dinosaurs (Bronzati et al., 2021). With the LSC horizontally aligned, the ASC projects further dorsally, and also posteriorly, in relation to the PSC; as a result, the common crus is posteriorly tilted. In dorsal view, an angle of ~80° is formed between the courses of the ASC and PSC at the level of the common crus. Additionally, whereas the ASC is mostly straight along its main course, the PCS is slightly bowed anteriorly, in a way that its posterior margin exhibits a concave aspect in lateral view. The anterior and lateral ampullae are clearly distinguishable from one another, as in *I. polesinensis* (ULBRA-PVT059). Parts of the vestibule and cochleae could be reconstructed for the right labyrinth, but no precise information can be extracted from this region



because of poor preservation. It is worth mentioning that this ventral portion of the labyrinth is not ossified in several stem-archosaurs, such as *E. capensis* (Sobral et al., 2016), and pseudosuchians (Gower, 2002; Gower & Nesbitt, 2006). Yet, the possibility to segment at least part of these structures is an indicator that this region was indeed partially ossified in *D. gregorii*.

## 4 | DISCUSSION

“Laterosphenoid” versus “Laterosphenoid + Orbitosphenoid.”

Based on their observations on the braincase of the non-archosaurian archosauriforms *P. alexanderi*, *Garjainia prima*, and *E. capensis*, Clark et al. (1993) presented a detailed discussion on the ossified elements that form the anterior region of the braincase in stem archosaurs. More recently, Sobral et al. (2016) brought back this topic after a reanalysis of the braincase of *E. capensis*. In these taxa, that anterior wall ossification has been associated with a single element, referred to as the laterosphenoid. In *E. capensis* (SAM-PK-5867) and *P. alexanderi* (Clark et al., 1993), the laterosphenoid is configured as an anteroposteriorly elongated (1.5–1.8 times longer than high) bone that contacts the prootic posteriorly, the parietal posterodorsally, and the frontal anterodorsally. Additionally, the posterior, dorsal, and anterior margins of the foramina associated to cranial nerves II to IV are formed by the laterosphenoid—the ventral margin of some of these foramina is likely not fully ossified in some archosaurs (e.g., Chapelle & Choiniere, 2018; Clark et al., 1993; Sobral et al., 2016).

Differently from the archosauriforms mentioned above, cranial nerves II–IV are fully enclosed by two bones on the anterior wall of the braincase in non-avian dinosaurs (e.g., Bronzati et al., 2019; Bronzati & Rauhut, 2017; Chapelle & Choiniere, 2018; Eddy & Clarke, 2011; Evans et al., 2009; Galton, 1985; Leahey et al., 2015; Sampson & Witmer, 2007). Studies on non-avian dinosaurs apply the term laterosphenoid to the bone that forms only the posterior margin of those foramina. Their anterior margins are formed by another ossified element of the anterior braincase wall, the orbitosphenoid. Further, the anterior margin of the orbitosphenoid typically also forms the posterior border of the foramen for cranial nerve II. In non-avian dinosaurs, the laterosphenoid contacts the prootic posteriorly, the parietal dorsally, and the frontal anterodorsally, whereas the orbitosphenoid contacts the laterosphenoid posteriorly and the frontal dorsally. The presence of an orbitosphenoid, anteromedially located in relation to the laterosphenoid, has also been reported for pterodactyloid

pterosaurs (Codorniu et al., 2016; Kellner, 1996). Kellner (1996) mentioned that the foramen for cranial nerve IV is completely enclosed by the laterosphenoid, whereas the foramina for cranial nerves II and III would be enclosed by laterosphenoid and orbitosphenoid together.

Thus, based on the position of the ossified elements in the braincase, their contact with other bones, and the position of foramina associated to ossified parts of the anterior braincase wall in archosauriforms, the “laterosphenoid,” as employed in previous studies of non-archosaurian archosauriforms (e.g., Clark et al., 1993; Sobral et al., 2016) is topologically equivalent to the “laterosphenoid + orbitosphenoid” of avemetatarsalians, such as non-avian dinosaurs and pterosaurs.

The braincase anatomy is not well known in early pterosaurs (Codorniu et al., 2016). In the non-pterodactyloid pterosaur *A. koi* (MPEF-PV 3613), a laterosphenoid is preserved, but its anterior extension is unknown because the portion of the braincase ventral to the anterior portion of the frontal is badly preserved. An orbitosphenoid seems absent in that taxon (Codorniu et al., 2016), but latero- and orbitosphenoids are unambiguously present in pterodactyloids (Kellner, 1996). Among early dinosaurs, laterosphenoids have been identified in *T. hallae* (GR 241), *B. schultzi* (CAPP/UFMS 0035), and *S. tupiniquim* (MCP 3845 PV). Except for *T. hallae* (GR 241), those taxa possess laterosphenoids that are similar to those of later-diverging dinosaurs and pterosaurs with orbitosphenoids, in which the laterosphenoid forms only the posterior margin of the foramina for cranial nerve IV. In *T. hallae* (GR 241) the situation is not clear, but the lack of an elongated anterior process of the laterosphenoid as observed in *P. alexanderi* (Clark et al., 1993) and *E. capensis* (SAM-PK-5867) indicates that it possessed a condition similar to that of other dinosaurs (as previously mentioned by Sobral et al., 2016). Regarding non-dinosaurian dinosauriforms, a laterosphenoid has been reported for *L. admixtus* (Bittencourt et al., 2014). However, the position of this putative laterosphenoid, i.e., anteroventral to the foramen for the trigeminal nerve (which is here also reinterpreted as the foramen for the facial nerve), is not consistent with the position of this bone in other dinosauriforms, i.e. anterodorsal to the trigeminal foramen. Our interpretation is that the structure reported in the holotype of *L. admixtus* as the laterosphenoid is instead a pendant process of the orbitosphenoidal crest, which also has a symmetric development on the right side of the braincase.

The presence of separated laterosphenoids and orbitosphenoids in a multitude of dinosaur and pterosaur specimens indicates that these elements were commonly ossified in these animals. There are multiple alternative scenarios that might explain the evolutionary patterns of

the “laterosphenoid + orbitosphenoid” of avemetatarsalians and the laterosphenoid of non-archosaurian archosauriforms (it is worth mentioning that pseudosuchians such as *Desmotosuchus* [Small, 2002] and *Stagonolepis* [Gower & Walker, 2002] exhibit a morphology that matches that observed in non-archosaurian taxa). The anterior braincase wall, ventral to the frontals, is formed by ossifications originating from distinct embryonic structures and cartilages (see details presented by Sampson & Witmer, 2007; Sobral et al., 2016). One possibility is that the non-archosaurian taxa mentioned here also possess an orbitosphenoid, but fusion of this bone with the laterosphenoid makes impossible to distinguish between them in taxa such as *E. capensis* (SAM-PK-5867) and *P. alexanderi* (Clark et al., 1993). Another possibility is that the laterosphenoid of non-archosaurian archosauromorphs and the laterosphenoid of avemetatarsalians result from the ossifications of different embryonic structures (e.g., pila metotica, pila antotica, taenia medialis). As discussed by Sobral et al. (2016; see also Bellairs & Kamal, 1981), the laterosphenoid of non-archosaurian amniotes might correspond to a more extensive ossification of the posterior and anterior portions of the “embryonic anterior wall of the braincase.” In this case, the laterosphenoid of avemetatarsalians could correspond to the ossification of the posterior/dorsal portion of the “embryonic anterior wall of the braincase,” whereas the orbitosphenoid from that of the “embryonic anterior wall of the braincase.”

Apart from the uncertainties regarding the osteological/developmental context discussed above, the early evolution of the anterior portion of the avemetatarsalian braincase is also difficult to be traced in a phylogenetic context. In early dinosaurs preserving a laterosphenoid (e.g., *T. hallae* [GR 241], *S. tupiniquim* [MCP 3845 PV], *B. schultzi* [CAPP/UFMS 0035]), this bone lacks the long anterior process observed in non-archosaurians and an orbitosphenoid is either absent or non-ossified. On the other hand, the elongated laterosphenoid anterior process present in TMM 31100-1334 (Figure 7) is more similar to that of non-archosaurian archosauromorphs than to that of early dinosaurs. This might indicate that the anterior region of the braincase had considerable variability in its degree of ossification soon after their split of the two main avemetatarsalian lineages, Pterosauroomorpha and Dinosauromorpha. However, the lack of more specimens preserving the anterior region of the braincase hampers a more detailed assessment of the evolution of these bones in the lineage.

The postparietal of TMM 31100-1334 in the phylogenetic context of Archosauromorpha.

In this study, we employed the term postparietal in reference to a distinct ossified element located between

the supraoccipital, posteriorly, and the parietals, anteriorly (Figures 2 and 4). Nevertheless, the terms interparietal or postparietal used in previous studies of archosauromorphs are equivalent (e.g., Ewer, 1965; Ezcurra, 2016; Gower, 1997; Sookias et al., 2020). The use of different names for this bone in previous studies is not related to their non-homologous nature but rather to the adoption of distinct nomenclature (see Koyabu et al., 2012). For instance, the term postparietal seems to be more frequently employed in the literature of early tetrapods, whereas the term interparietal seems more common among works on extant mammals (Koyabu et al., 2012). Alternatively, Ezcurra (2016) treated the interparietal as the element formed by the fusion of paired postparietals in archosauromorphs. However, the term postparietal has been previously employed both for paired and unpaired elements (Klembara, 2001; Romer, 1956). Additionally, Klembara (2001) mentioned that the interparietal of mammals and the postparietal of *Alligator mississippiensis* are topologically equivalent and possibly homologous, either in a paired or an unpaired condition.

In some taxa lacking a postparietal, such as the dinosaurs *B. schultzi* (CAPP/UFMS 0035), *H. ischigualastensis* (PVSJ 407), and *P. engelhardti* (SMNS 13200; AMNH 6810), there is a gap medially located between the supraoccipital and parietals, the postparietal foramen (=postparietal fenestra). This does not seem to be the case in the ornithischian dinosaur *H. tucki* (SAM-PK-K337), in which the anterodorsal margin of the supraoccipital contacts the medial portion of the posterior margin of the parietal. A postparietal was coded as present in the Brazilian lagerpetid *I. polesinensis* (ULBRA-PVT059) in the phylogenetic study of Cabreira et al. (2016), but further analyses indicate that the postparietal is not known for this taxon (Ezcurra et al., 2020; M.B. pers. obs.). Three-dimensional reconstruction of the *I. polesinensis* skull (see Ezcurra et al., 2020) indicate that, in the absence of a postparietal bone, a postparietal foramen could also be present. Given the morphological similarity between the shape of the parietals and supraoccipital of both lagerpetids *I. polesinensis* (ULBRA-PVT059) and TMM 31100-1334 (as described here), we interpret that the ossification located medially between the parietal and supraoccipital indeed corresponds to a postparietal. An alternative scenario, with this ossification considered as part of either the parietal or the supraoccipital, would imply rather different morphologies for both bones, strikingly different from that of any other archosauromorph.

A postparietal is present in non-archosaurian archosauromorphs such as *E. capensis* (Ewer, 1965; Sookias et al., 2020), *Tasmaniosaurus triassicus* (Ezcurra, 2014), and *E. africanus* (Gower, 1997), in which the bone is located between the base of the posterolaterally diverging rami of the parietal wings. Gauthier (1984) first proposed the

absence of a postparietal (=interparietal) as synapomorphic for Archosauriformes, whereas Benton & Clark (1988) proposed the absence of this bone as synapomorphic for Archosauria. Nevertheless, as already explained by Bennett (1996), this difference is because the postparietal-bearing *E. capensis* was treated as a member of Archosauria by Gauthier (1984), but regarded as a non-archosaurian archosauriform by Benton & Clark (1988).

The presence of a postparietal among archosaurs is so far confirmed only for early ontogenetic stages of the living species *Alligator mississippiensis* (Klembara, 2001). Thus, the presence of this bone in TMM 31100-1334 corresponds to the only evidence of this bone among extinct crown-group archosaurs so far. The postparietal of TMM 31100-1334 most likely corresponds to a single element, which is the condition observed in saurians, unlike diapsids such as *Youngina capensis* and *Petrolacosaurus kanensis* that exhibit paired elements (Ezcurra, 2016). Thus, in the context of archosauromorph evolution, the only variation is related to the presence/absence of a postparietal in its different subgroups (Ezcurra, 2016).

Multiple scenarios can be proposed to explain the presence of a postparietal in TMM 31100-1334. One is that its condition corresponds to the retention of the ancestral Archosauromorpha state in early members of Pterosauriformes. In this case, the loss of the postparietal in Pterosauria and Dinosauriformes would correspond to independent events. A second scenario is that the absence of the postparietal in the latter groups results from the loss of this bone at the base of Avemetatarsalia. Hence, its presence in TMM 31100-1334 would correspond to an independent reacquisition within Archosauromorpha. However, the scenario concerning the evolution of the postparietal can be much more complex, not following a “parsimonious” pattern. As demonstrated for extant tetrapods (e.g., Klembara, 2001; Koyabu et al., 2012), the elements at the occipital region of the skull related to the postparietal of non-archosaurian archosauriforms might fuse with other elements early in ontogeny. Thus, in lineages such as Dinosauria, where a separate postparietal is not observed, it is possible that this bone fuses with the supraoccipital and/or parietal in early ontogenetic stages. In this sense, more detailed studies on the ontogeny of extant archosaurs (e.g., Klembara, 2001) might provide a clearer scenario for the evolution of the postparietal in the group.

#### 4.1 | The basitubera of early archosauromorphs

The basitubera are typically represented by protuberances and/or ridges in the basioccipital and/or parabasioccipital that correspond to attachment areas for the

craniocervical musculature, with the number and shape of protuberances/ridges varying among different groups of vertebrates (Romer, 1956; Snively & Russell, 2007). As seen in TMM 31100-1334, a basisphenoid component of the basitubera located on the postero-lateroventral corner of the parabasioccipital is common to all dinosauriforms, pterosaurs, pseudosuchians, and non-archosaurian archosauromorphs observed for this study (Table 1), indicating that this shape is conservative among archosauromorphs. A higher variation is, however, observed in the basioccipital component of the basitubera.

As described above, TMM 31100-1334 has a medial component of the basioccipital basitubera that is composed by a central protuberance and two ridges forming a V-shape structure, as well as lateral components that take the shape of knobs (protuberances), which are posterodorsally located in relation to the medial component (Figures 5 and 6). Among the taxa of our sample a ridge-like medial component is also observed in the non-archosaurian archosauriform *T. primus* (TMM 31100-1030), the pterosaur *A. koi* (MPEF-PV 3613), and in the sauropodomorph *E. minor* (Bronzati & Rauhut, 2017). Nevertheless, differences are also observed among these taxa. Whereas *T. primus* and *A. koi* exhibit a V-shaped ridge with an anteroposterior elongation, as in TMM 31100-1334, the sauropodomorph *E. minor* possesses a transverse ridge. More broadly speaking, a ridge-like medial component of the basioccipital basitubera differs from the condition most typically seen in the taxa of our sample, which corresponds to two protuberances, clearly separated at midline, as seen in the non-archosaurian archosauriform *E. capensis* (SAM-PK-7696; SAM-PK-5867), the pseudosuchians *P. gracilis* (NMT RB426) and *Arizonasaurus babbitti* (MSM P459), the non-dinosaurian dinosauriforms *L. admixtus* (PULR-V 01) and *L. talampayensis* (PVL 3872), the herrerasaurid *H. ischigualastensis* (PVSJ 407), and the neotheropod *M. rhodesiensis* (QG 195, QG 197). Yet, differentiating between the two conditions mentioned above—that is, a ridge or two separated protuberances—is not always straightforward. For instance, in the sauropodomorphs *T. antiquus* (Bronzati & Rauhut, 2017) and *P. engelhardti* (MB.R.5586-1; SMNS 13200; AMNH 6810), and the ornithischian *L. diagnosticus* (NHMUK PV R8501), a depression is observed in the midline of the medial component of the basitubera, but our interpretation is that these taxa also exhibit a ridge-like structure, as evidenced by the connection in the posterior portion of the medial component of the basioccipital basitubera. One likely scenario is that a ridge-like medial component of the basioccipital basitubera results from the fusion/merging of the protuberance-like components. It is worth mentioning that the ridge in the medial component of the basioccipital



basitubera is not homologous to the intertuberal plate of some non-archosaurian archosauromorphs (e.g., Gower & Sennikov, 1996), which corresponds to a connection between the basitubera components of the basisphenoid. As mentioned by Nesbitt (2011), crown-group archosaurs lack the basisphenoid plate.

Another variation regarding the basitubera is related to the presence of lateral protuberances such as those described here for TMM 31100-1334 and also found in the non-archosaurian archosauriform *T. primus* (TMM 31100-1030), the sauropodomorphs *P. engelhardti* (MB. R.5586-1; SMNS 13200; AMNH 6810) and *B. schultzi* (CAPP/UFMS 0035), and the pseudosuchian *B. kupferzellensis*. Gower (2002) considered the basioccipital basitubera of the latter taxon as bilobate, which is equivalent to our definition of a medial and a lateral component on each side of the braincase. Differently, no lateral protuberance is observed in the non-archosaurian archosauriform *E. capensis* (SAM-PK-7696; SAM-PK-5867), the pseudosuchian *P. gracilis* (NMT RB426), the non-dinosaurian dinosauromorphs *L. admixtus* (PULR-V 01) and *L. talampayensis* (PVL 3872), the silesaurid *S. opoleensis* (ZPAL Ab III/361; ZPAL Ab III/362), and the theropod *E. murphi* (PVSJ 562). Thus, as detailed above for the configuration of the medial element, the presence/absence of these protuberances is also highly variable among archosauromorphs. This might reflect, for instance, the co-optation of distinct muscle groups in animals with different neck mobilities. Another possibility concerns the presence or absence of a distinct craniocervical musculature among different groups (e.g., Bronzati et al., 2018). However, the absence of lateral protuberances might not be a strong indication for less muscles attached to the occipital region of the basioccipital, as a muscle could still attach in flat surfaces of the basioccipital and/or parabasisphenoid (see e.g., Snively & Russell, 2007).

## 4.2 | Sensory systems

Features of the brain and semicircular canals of lagerpetids have been identified as intermediate between those of pterosaurs and other archosaurs (Ezcurra et al., 2020); with 3D geometric morphometric analyses revealing that the overall shape of the semicircular canals of *D. gregorii* and *I. polesinensis* (ULBRA-PVT059) is more similar to that of pterosaurs than to that of other archosauromorphs (Bronzati et al., 2021). Both lagerpetids and pterosaurs exhibit a circular ASC, which is also observed in birds (e.g., Benson et al., 2017). Nevertheless, a more circular ASC is also observed among non-flying archosauromorphs (see Bronzati et al., 2021); thus the resemblance

of the ASCs among lagerpetids, pterosaurs, and birds mostly likely results from constraints imposed by the braincase shape in the form of the labyrinth rather than from any functional adaptation (Bronzati et al., 2021). Additional support for the latter claim comes from biomechanical studies on inner ear function. Modifications in the shape of the SCCs have minimal impact on their sensitivity (David et al., 2010); in a way that the use of 3D geometric morphometrics to quantify canal function can be deeply flawed. This is because it transforms the morphological signal of the SCCs in a way that is not compatible with biomechanical functional models (David et al., 2022). In this case, one possibility is that the presence of a more circular ASC in taxa such as lagerpetids and pterosaurs is the result of the enlarged floccular fossa.

The floccular lobe of the cerebellum in lagerpetids extends into the space within the semicircular canals. Together with pterosaurs, they represent the only archosauromorphs in which the height of the base of the floccular lobe corresponds to 0.4 (or more) of that of the endocast in this region (Ezcurra et al., 2020). However, it is difficult to precisely estimate the relative volume of the floccular lobe in lagerpetids, given that the brain endocast of *D. gregorii* is greatly deformed, and that of *I. polesinensis* (ULBRA-PVT059) is mostly incomplete. Additionally, despite suggestions that the relative size of the flocculus might carry functional significance for the ecology of archosaurs (Bronzati et al., 2017; Lautenschlager et al., 2012; Witmer et al., 2003), apart from the presence of relatively larger flocculus among predatory birds (Ferreira-Cardoso et al., 2017), no clear statistical association between flocculus size and a particular behavior has been yet established. Thus, it is so far difficult to trace a more detailed scenario on the evolution of the floccular fossa in early archosauromorphs, and hence establishing any possible link between changes in the volume of this structure with the evolution of distinct types of behavior in these taxa.

## 5 | CONCLUSIONS

Cranial materials of lagerpetids are rare elements, and so far no complete skull is known for these enigmatic animals. The braincase of *D. gregorii* described here represents the first effort to document their cranial anatomy, helping to understand the transformations that happened in the skull of early avemetatarsalians. The braincase shape of specimen TMM 31100-1334 deviates from that of other avemetatarsalians by the presence of a postparietal, so far unknown in any other extinct taxa of the archosaur crown-group, and by the presence of an anteroposteriorly-elongated laterosphenoid forming the

whole anteroventral portion of the braincase, thus lacking the orbitosphenoid as seen in other avemetatarsalians. The endocast of TMM 31100-1334 shows that lagerpetids share with pterosaurs traits in structures related to the sensory systems. *Dromomeron gregorii* had a hypertrophied floccular lobe of the cerebellum, a condition that is even further exacerbated in the flying pterosaurs (Ezcurra et al., 2020), and large semicircular canals, with the anterior canal exhibiting a circular shape; also typical of pterosaurs. This scenario might suggest that the shape of the sensory structures of lagerpetids corresponds to an intermediate shape related to the acquisition of flight in pterosaurs (see e.g., Ezcurra et al., 2020). Nevertheless, tentative association between the shape of the components of the sensory systems with any ecological trait remains tentative and should be taken with caution (see e.g., Bronzati et al., 2017, 2020; David et al., 2022; Ferreira-Cardoso et al. 2017; Walsh et al., 2013).

#### AUTHOR CONTRIBUTIONS

**Mario Bronzati:** Conceptualization; formal analysis; funding acquisition; investigation; methodology; validation; visualization; writing – original draft; writing – review and editing. **Max C. Langer:** Funding acquisition; investigation; project administration; supervision; visualization; writing – review and editing. **Martín D. Ezcurra:** Formal analysis; investigation; writing – review and editing. **Michelle R. Stocker:** Data curation; funding acquisition; project administration; investigation; resources, writing – review and editing. **Sterling J. Nesbitt:** Conceptualization; data curation; formal analysis; investigation; methodology; resources; supervision; validation; visualization; writing – original draft; writing – review and editing.

#### ACKNOWLEDGMENTS

We are thankful to Matthew W. Colbert for assistance with CT imaging and to Larry M. Witmer for scientific advice. M. Brown and J.C. Sagebiel provided access to the specimen, preparation advice, and curatorial advice. D. Abelin, J. Powell, R. Schoch, R. Martínez, and Z. Erasmus helped and/or provided access to materials in collections, which we are thankful for. We are especially thankful to the reviewers Gabriela Sobral and Rodrigo T Müller for their insightful comments. Open Access funding enabled and organized by Projekt DEAL.

#### CONFLICT OF INTEREST STATEMENT


The authors have no conflicts of interest to declare.


#### DATA AVAILABILITY STATEMENT

CT data of the specimen TMM 31100-1334 are available at the public repository MorphoSource: <https://www.morphosource.org/projects/000535758>.

#### ORCID

Mario Bronzati  <https://orcid.org/0000-0003-1542-3199>

Martín D. Ezcurra  <https://orcid.org/0000-0002-6000-6450>

Sterling J. Nesbitt  <https://orcid.org/0000-0002-7017-1652>

#### REFERENCES

- Arcucci, A. (1986). New materials and reinterpretation of *Lagerpeton chanarensis* Romer (Thecodontia, Lagerpetonidae nov.) from the Middle Triassic of La Rioja, Argentina. *Ameghiniana*, 23, 233–242.
- Baron, M. G. (2021). The origin of pterosaurs. *Earth Science Reviews*, 221, 103777.
- Bellairs, A., & Kamal, A. M. (1981). The chondrocranium and the development of the skull in recent reptiles. In C. Gans & T. S. Parsons (Eds.), *Biology of the Reptilia, volume 11, morphology F* (pp. 1–283). Academic Press.
- Bennett, S. C. (1996). The phylogenetic position of the Pterosauria within the Archosauromorpha. *Zoological Journal of the Linnean Society*, 118, 261–308.
- Benson, R. B. J., Starmer-Jones, E., Close, R. A., & Walsh, S. A. (2017). Comparative analysis of vestibular ecomorphology in birds. *Journal of Anatomy*, 231, 990–1018.
- Benton, M. J., & Clark, J. M. (1988). Archosaur phylogeny and the relationships of the Crocodylia. In M. J. Benton (Ed.), *The phylogeny and classification of the tetrapods. Volume 1. Amphibians, reptiles, birds The Systematics Association Special Volume No. 35A* (pp. 295–338). Clarendon Press.
- Bittencourt, J. S., Arcucci, A. B., Marsicano, C. A., & Langer, M. C. (2014). Osteology of the Middle Triassic archosaur *Lewisuchus admixtus* Romer (Chañares Formation, Argentina), its inclusivity, and relationships amongst early dinosauromorphs. *Journal of Systematic Palaeontology*, 13, 189–219.
- Britt, B. B., Dalla Vecchia, F. M., Chure, D. J., Engelmann, G. F., Whiting, M. F., & Scheetz, R. D. (2018). *Caelestiventus hanseni* gen. et sp. nov. extends the desert-dwelling pterosaur record back 65 million years. *Nature Ecology & Evolution*, 2, 1386–1392.
- Bronzati, M., Benson, R. B. J. & Rauhut, O. W. M. (2018). Rapid transformation in the braincase of sauropod dinosaurs: integrated evolution of the braincase and neck in early sauropods? *Palaeontology*, 61, 289–302.
- Bronzati, M., Benson, R. B. J., Evers, S. W., Ezcurra, M. D., Cabreira, S. F., Choiniere, J., Dollman, K. N., Paulina-Carabajal, A., Radermacher, V. J., da Silva, L. R., Sobral, G., Stocker, M. R., Witmer, L. M., Langer, M. C., & Nesbitt, S. J. (2021). Deep evolutionary diversification of archosaur locomotion reflected by vestibular morphology. *Current Biology*, 31, 2520–2529.
- Bronzati, M., Langer, M. C., & Rauhut, O. W. M. (2019). Braincase anatomy of the early sauropodomorph *Saturnalia tupiniquim* (Late Triassic, Brazil). *Journal of Vertebrate Paleontology*, e1559173. <https://doi.org/10.1080/02724634.2018.1559173>
- Bronzati, M., & Rauhut, O. W. M. (2017). Braincase redescription of *Efraasia minor* Huene, 1908 (Dinosauria: Sauropodomorpha) from the Late Triassic of Germany, with comments on the evolution of the sauropodomorph braincase. *Zoological Journal of the Linnean Society*, 182, 173–224.

- Bronzati, M., Rauhut, O. W. M., Bittencourt, J. S., & Langer, M. C. (2017). Endocast of the Late Triassic (Carnian) dinosaur *saturnalia tupiniquim*: Implications for the evolution of brain tissue in Sauropodomorpha. *Scientific Reports*, 7, 11931.
- Busbey, A. B. (1989). Form and function of the feeding apparatus of *Alligator mississippiensis*. *Journal of Morphology*, 202, 99–127.
- Cabreira, S. F., Kellner, A. W. A., Dias-Da-Silva, S., Silva, L. R., Bronzati, M., Marsola, J. C. A., Müller, R. T., Bittencourt, J. S., Batista, B. J., Raugust, T., Carrilho, R., Brodt, A., & Langer, M. C. (2016). A unique Late Triassic dinosauromorph assemblage reveals dinosaur ancestral anatomy and diet. *Current Biology*, 26, 3090–3095.
- Chapelle, K. E. J., & Choiniere, J. N. (2018). A revised cranial description of *Massospondylus carinatus* Owen (Dinosauria: Sauropodomorpha) based on computed tomographic scans and a review of cranial characters for basal Sauropodomorpha. *PeerJ*, 6, e4224.
- Chure, D. J., & Madsen, J. H. (1996). Variation in aspects of the tympanic pneumatic system in a population of *Allosaurus fragilis* from the Morrison Formation (Upper Jurassic). *Journal of Vertebrate Paleontology*, 16, 573–577.
- Clark, J. M., Welman, J., Gauthier, J. A., & Parrish, J. M. (1993). The laterosphenoid bone of early archosauriforms. *Journal of Vertebrate Paleontology*, 13, 48–57.
- Codorniú, L., Paulina-Carabajal, A., Pol, D., Unwin, D., & Rauhut, O. W. M. (2016). A Jurassic pterosaur from Patagonia and the origin of the pterodactyloid neurocranium. *PeerJ*, 4, e2311.
- David, R., Bronzati, M., & Benson, R. B. J. (2022). Comment on “The early origin of a birdlike inner ear and the evolution of dinosaurian movement and vocalization”. *Science* 376:eabl7610, 376, eabl7610.
- David, R., Droulez, J., Allain, R., Berthoz, A., Janvier, P., & Bennequin, D. (2010). Motion from the past: A new method to infer vestibular capacities of extinct species. *Comptes Rendus Palevol*, 9, 367–410.
- Eddy, D. R., & Clarke, J. A. (2011). New information on the cranial anatomy of *Acrocanthosaurus atokensis* and its implications for the phylogeny of Allosauroida (Dinosauria: Theropoda). *PLoS One*, 6, e17932.
- Evans, D. C., Ridgely, R., & Witmer, L. M. (2009). Endocranial anatomy of lambeosaurine hadrosaurids (Dinosauria: Ornithischia): A sensorineural perspective on cranial crest function. *The Anatomical Record*, 292, 1315–1337.
- Ewer, R. F. (1965). The anatomy of the thecodont reptile *Euparkeria capensis* broom. *Philosophical Transactions of the Royal Society B, Biological Sciences*, 248, 379–435.
- Ezcurra, M. D. (2014). The osteology of the basal archosauriform *Tasmaniosaurus triassicus* from the Lower Triassic of Tasmania, Australia. *PLoS One*, 9, e86864.
- Ezcurra, M. D. (2016). The phylogenetic relationships of basal archosauriforms, with an emphasis on the systematics of proterosuchian archosauriforms. *PeerJ*, 4, e1778.
- Ezcurra, M. D., & Butler, R. J. (2015). Taxonomy of the proterosuchid archosauriforms (Diapsida: Archosauromorpha) from the earliest Triassic of South Africa, and implications for the early archosauriform radiation. *Palaeontology*, 58, 141–170.
- Ezcurra, M. D., Nesbitt, S. J., Bronzati, M., Dalla Vecchia, F. M., Agnolin, F. L., Benson, R. B. J., Brissón Egli, F., Cabreira, S. F., Evers, S. W., Gentil, A. R., Irmis, R. B., Martinelli, A. G., Novas, F. E., Roberto-da-Silva, L., Smith, N. D., Stocker, M. R., Turner, A. H., & Langer, M. C. (2020). Enigmatic dinosaur precursors bridge the gap to the origin of Pterosauria. *Nature*, 588, 445–449.
- Ferreira-Cardoso, S., Araújo, R., Martins, N. E., Martins, G. G., Walsh, S., Martins, R. M. S., Kardjilov, M., Hilger, A., & Castaninha, R. (2017). Floccular fossa size is not a reliable proxy of ecology and behaviour in vertebrates. *Scientific Reports*, 7, 2005.
- Foffa, D., Dunne, E. M., Nesbitt, S. J., Butler, R. J., Fraser, N. C., Brusatte, S. L., Farnsworth, A., Lunt, D. J., Valder, P. J., Walsh, S., & Barrett, P. M. (2022). *Scleromochlus* and the early evolution of Pterosauria. *Nature*, 610, 313–318.
- Galton, P. M. (1985). Cranial anatomy of the prosauropod dinosaur *Plateosaurus* from the Knollenmergel (Middle Keuper, Upper Triassic) of Germany. II. All the cranial material and details of soft-part anatomy. *Geologica et Palaeontologica*, 19, 119–159.
- Gardner, N. M., Holliday, C. M., & O’Keefe, F. R. (2010). The braincase of *Youngina capensis* (Reptilia, Diapsida): New insights from high-resolution CT scanning of the holotype. *Palaeontologia Electronica*, 13, 19A.
- Gasparini, Z., Fernández, M., & de la Fuente, M. (2004). A new pterosaur from the Jurassic of Cuba. *Palaeontology*, 47, 919–927.
- Gauthier, J. A. (1984). *A cladistic analysis of the higher systematic categories of the Diapsida* (Ph.D. dissertation). University of California, Berkeley, 1128.
- George, I. D., & Holliday, C. M. (2013). Trigeminal nerve morphology in *Alligator mississippiensis* and its significance for crocodyliform facial sensation and evolution. *The Anatomical Record*, 296, 670–680.
- Gower, D. J. (1997). The braincase of the early archosaurian reptile *Erythrosuchus africanus*. *Journal of Zoology*, 242, 557–576.
- Gower, D. J. (2002). Braincase evolution in suchian archosaurs (Reptilia: Diapsida): Evidence from the raiusuchian *Batrachotomus kupferzellensis*. *Zoological Journal of the Linnean Society*, 136, 49–76.
- Gower, D. J., & Nesbitt, S. J. (2006). The braincase of *Arizonasaurus babbitti*—Further evidence for the non-monophyly of ‘Raiusuchian’ archosaurs. *Journal of Vertebrate Paleontology*, 26, 79–87.
- Gower, D. J., & Sennikov, A. G. (1996). Morphology and phylogenetic informativeness of early archosaur braincases. *Palaeontology*, 39, 883–906.
- Gower, D. J., & Walker, A. D. (2002). New data on the braincase of the aetosaurian archosaur (Reptilia: Diapsida) *Stagonolepis robertsoni* Agassiz. *Zoological Journal of the Linnean Society*, 136, 7–23.
- Gower, D. J., & Weber, E. (1998). The braincase of *Euparkeria*, and the evolutionary relationships of avialans and crocodylians. *Biological Reviews*, 73, 367–411.
- Holliday, C. M. (2009). New insights into dinosaur jaw muscle anatomy. *The Anatomical Record*, 292, 1246–1265.
- Holliday, C. M., & Witmer, L. M. (2009). The epipterygoid of crocodyliforms and its significance for the evolution of the orbito-temporal region of eusuchians. *Journal of Vertebrate Paleontology*, 29, 715–733.
- Irmis, R. B., Nesbitt, S. J., Padian, K., Smith, N. D., Turner, A. H., Woody, D., & Downs, A. (2007). A Late Triassic dinosauromorph assemblage from New Mexico and the rise of dinosaurs. *Science*, 317, 358–361.
- Kammerer, C. F., Nesbitt, S. J., Flynn, J. J., Ranivoharimanana, L., & Wyss, A. R. (2020). A tiny ornithomimid archosaur from the Triassic of Madagascar and the role of



- miniaturization in dinosaur and pterosaur ancestry. *Proceedings of the National Academy of Sciences*, 117, 17932–17936.
- Kellner, A. W. A. (1996). Description of the braincase of two Early Cretaceous pterosaurs (Pterodactyloidea) from Brazil. *American Museum Novitates*, 3175, 1–34.
- Kellner, A. W. A., Holgado, B., Grillo, O., Pretto, F. Z., Kerber, L., Pinheiro, F. L., Soares, M. B., Schultz, C. L., Lopes, R. T., Araújo, O., & Müller, R. T. (2022). Reassessment of *Faxinalipterus minimus*, a purported Triassic pterosaur from southern Brazil with the description of a new taxon. *PeerJ*, 10, e13276.
- Klembara, J. (2001). Postparietal and prehatching ontogeny of the supraoccipital in *Alligator mississippiensis* (Archosauria, Crocodylia). *Journal of Morphology*, 249, 147–153.
- Koyabu, D., Maier, W., & Sánchez-Villagra, M. (2012). Paleontological and developmental evidence resolve the homology and dual embryonic origin of a mammalian skull bone, the interparietal. *Proceedings of the National Academy of Sciences*, 109, 14075–14080.
- Leahey, L. G., Molnar, R. E., Carpenter, K., Witmer, L. M., & Salisbury, S. W. (2015). Cranial osteology of the ankylosaurian dinosaur formerly known as *Minmi* sp. (Ornithischia: Thyreophora) from the Lower Cretaceous Allaru Mudstone of Richmond, Queensland, Australia. *PeerJ*, 3, e1475.
- Martínez, R. N., Apaldetti, C., Correa, G. A., & Abelin, D. (2016). A Norian lagerpetid dinosauriform from the Quebrada del Barro Formation, northwestern Argentina. *Ameghiniana*, 53, 1–13.
- Martínez, R. N., Haro, J. A., & Apaldetti, C. (2012). Braincase of *Panphagia protos* (Dinosauria, Sauropodomorpha). *Journal of Vertebrate Paleontology*, 32(Suppl. 1), 70–82.
- Müller, R. T., Ezcurra, M. D., Garcia, M. S., Agnolin, F. L., Stocker, M. R., Novas, F. E., Soares, M. B., Kellner, A. W. A., & Nesbitt, S. J. (2023). New reptile shows dinosaurs and pterosaurs evolved among diverse precursors. *Nature*, 620, 589–594.
- Müller, R. T., Ferreira, J. D., Pretto, F. A., Bronzati, M., & Kerber, L. (2020). The endocranial anatomy of *Buriolestes schultzi* (Dinosauria: Saurischia) and the early evolution of brain tissues in sauropodomorph dinosaurs. *Journal of Anatomy*, 238, 809–827.
- Nesbitt, S. J. (2011). The early evolution of archosaurs: Relationships and the origin of major clades. *Bulletin of the American Museum of Natural History*, 352, 1–292.
- Nesbitt, S. J., Irmis, R. B., Parker, W. G., Smith, N. D., Turner, A. H., & Rowe, T. (2009). Hindlimb osteology and distribution of basal dinosauriforms from the Late Triassic of North America. *Journal of Vertebrate Paleontology*, 29, 498–516.
- Nesbitt, S. J., Smith, N. D., Irmis, R. B., Turner, A. H., Downs, A., & Norell, M. A. (2009). A complete skeleton of a Late Triassic saurischian and the early evolution of dinosaurs. *Science*, 326, 1530–1533.
- Nesbitt, S. J., Stocker, M. R., Parker, W. G., Wood, T. A., Sidor, C. A., & Angielczyk, K. D. (2018). The braincase and endocast of *Parringtonia gracilis*, a Middle Triassic suchian (Archosauria: Pseudosuchia). *Journal of Vertebrate Paleontology*, 37(Suppl. 1), 122–141.
- Novas, F. E. (1996). Dinosaur monophyly. *Journal of Vertebrate Paleontology*, 16, 723–741.
- Pinheiro, F. L., França, M. A. G., Lacerda, M. B., Butler, R. J., & Schultz, C. L. (2016). An exceptional fossil skull from South America and the origins of the archosauriform radiation. *Scientific Reports*, 6(1). <https://doi.org/10.1038/srep22817>
- Porro, L. B., Witmer, L. M., & Barrett, P. M. (2015). Digital preparation and osteology of the skull of *Lesothosaurus diagnosticus* (Ornithischia, Dinosauria). *PeerJ*, 3, e1494.
- Rauhut, O. W. M. (2003). The interrelationships and evolution of basal theropod dinosaurs. *Special Papers in Palaeontology*, 69, 1–213.
- Rauhut, O. W. M. (2004). Braincase structure of the Middle Jurassic theropod dinosaur *Piatnitzkysaurus*. *Canadian Journal of Earth Sciences*, 41, 1109–1122.
- Romer, A. S. (1956). *Osteology of the reptiles* (p. 772). University of Chicago Press.
- Romer, A. S. (1971). The Chañares (Argentina) Triassic reptile fauna. X. Two new but incompletely known long-limbed pseudosuchians. *Breviora*, 378, 1–10.
- Sampson, S. D., & Witmer, L. M. (2007). Craniofacial anatomy of *Majungasaurus crenatissimus* (Theropoda: Abelisauridae) from the Late Cretaceous of Madagascar. *Journal of Vertebrate Paleontology*, 27, 32–102.
- Sereno, P. C. (1991). Basal archosaurs: Phylogenetic relationships and functional implications. *Memoir of the Society of Vertebrate Paleontology*, 2, 1–53.
- Sereno, P. C., & Arcucci, A. B. (1993). Dinosaurian precursors from the Middle Triassic of Argentina: *Lagerpeton chanarensis*. *Journal of Vertebrate Paleontology*, 13, 385–399.
- Sereno, P. C., & Novas, F. E. (1994). The skull and neck of the basal theropod *Herrerasaurus ischigualastensis*. *Journal of Vertebrate Paleontology*, 13, 451–476.
- Small, B. J. (2002). Cranial anatomy of *Desmatosuchus haplocerus* (Reptilia: Archosauria: Stagonolepididae). *Zoological Journal of the Linnean Society*, 136, 97–111.
- Snively, E., & Russell, A. P. (2007). Functional morphology of neck musculature in the Tyrannosauridae (Dinosauria, Theropoda) as determined via a hierarchical inferential approach. *Zoological Journal of the Linnean Society*, 151, 759–808.
- Sobral, G., & Müller, J. (2019). The braincase of *Mesosuchus browni* (Reptilia, Archosauromorpha) with information on the inner ear and description of a pneumatic sinus. *PeerJ*, 7, e6798.
- Sobral, G., Sookias, R. B., Bhullar, B.-A. S., Smith, R., Butler, R. J., & Müller, J. (2016). New information on the braincase and inner ear of *Euparkeria capensis* broom: Implications for diapsid and archosaur evolution. *Royal Society Open Science*, 3, 160072.
- Sookias, R. B., Dilkes, D., Sobral, G., Smith, R. M. H., Wolvaardt, F. P., Arcucci, A. B., Bhullar, B.-A. S., & Werneburg, I. (2020). The craniomandibular anatomy of the early archosauriform *Euparkeria capensis* and the dawn of the archosaur skull. *Royal Society Open Science*, 7, 200116.
- Stocker, M. R. (2013). *Contextualizing vertebrate faunal dynamics: new perspectives from the Triassic and Eocene of Western North America*. PhD Dissertation. University of Texas at Austin. 297 p.
- Stocker, M. R., Nesbitt, S. J., Criswell, K. E., Parker, W. G., Witmer, L. M., Rowe, T. B., Ridgely, R. C., & Brown, M. A. (2016). A dome-headed stem-archosaur exemplifies convergence among dinosaurs and their distant relatives. *Current Biology*, 26, 2676–2680.
- Tschopp, E., Mateus, O., & Benson, R. B. J. (2015). A specimen-level phylogenetic analysis and taxonomic revision of Diplodocidae (Dinosauria, Sauropoda). *PeerJ*, 3, e857.
- Walker, A. D. (1990). A revision of *Sphenosuchus acutus* Houghton, a crocodylomorph reptile from the Elliot Formation (Late Triassic or Early Jurassic) of South Africa.

- Philosophical Transactions of the Royal Society B: Biological Sciences*, 330, 1–120.
- Walsh, S. A., Iwaniuk, A. N., Knoll, M. A., Bourdon, E., Barrett, P. M., Milner, A. C., Nudds, R. L., Abel, R. L., & Sterpaio, P. D. (2013). Avian cerebellar floccular fossa size is not a proxy for flying ability in birds. *PLoS One*, 8, e67176.
- Witmer, L. M. (1997). Craniofacial air sinus systems. In P. J. Currie & K. Padian (Eds.), *Encyclopedia of dinosaurs* (pp. 151–159). Academic Press.
- Witmer, L. M., Chatterjee, S., Franzosa, J., & Rowe, T. (2003). Neuroanatomy of flying reptiles and implications for flight, posture and behaviour. *Nature*, 425, 950–953.
- Witmer, L. M., Ridgely, R. C., Dufeu, D. L., & Semones, M. C. (2008). Using CT to peer into the past: 3D visualization of the brain and ear regions of birds, crocodiles, and nonavian dinosaurs. In H. Endo & R. Frey (Eds.), *Anatomical imaging: Towards a new morphology* (pp. 67–87). Springer-Verlag.

**How to cite this article:** Bronzati, M., Langer, M. C., Ezcurra, M. D., Stocker, M. R., & Nesbitt, S. J. (2023). Braincase and neuroanatomy of the lagerpetid *Dromomeron gregorii* (Archosauria, Pterosauriformes) with comments on the early evolution of the braincase and associated soft tissues in Avemetatarsalia. *The Anatomical Record*, 1–28. <https://doi.org/10.1002/ar.25334>